LEVEL

(12)

AD A070040

TECHNICAL REPORT RR-7T-2

NOISE IN COHERENT OPTICAL SYSTEMS: MINIMUM DETECTABLE OBJECT CONTRAST AND SPECKLE SMOOTHING

C. R. Christensen
B. D. Guenther
J. S. Bennett
Physical Sciences Directorate
and
Nicholas George
California Institute of Technology
Pasadena, California 91125

19 July 1976

U.S. ARMY MISSILE COMMAND
Redstone Arsenal, Alabama 35809

DISPOSITION INSTRUCTIONS

DESTROY THIS REPORT WHEN IT IS NO LONGER NEEDED. DO NOT RETURN IT TO THE ORIGINATOR.

DISCLAIMER

THE FINDINGS IN THIS REPORT ARE NOT TO BE CONSTRUED AS AN OFFICIAL DEPARTMENT OF THE ARMY POSITION UNLESS SO DESIGNATED BY OTHER AUTHORIZED DOCUMENTS.

TRADE NAMES

USE OF TRADE NAMES OR MANUFACTURERS IN THIS REPORT DOES NOT CONSTITUTE AN OFFICIAL ENDORSEMENT OR APPROVAL OF THE USE OF SUCH COMMERCIAL HARDWARE OR SOFTWARE.

UNCLASSIFIED
SECURITY CLASSIFICATION OF THIS PAGE (When Data Entered)

REPORT DOCUMENTATION PAGE

READ INSTRUCTIONS BEFORE COMPLETING FORM

1. REPORT NUMBER: TR-RR-7T-2
2. GOVT ACCESSION NO.
3. RECIPIENT'S CATALOG NUMBER: (9)

4. TITLE (and Subtitle): (6) NOISE IN COHERENT OPTICAL SYSTEMS: MINIMUM DETECTABLE OBJECT CONTRAST AND SPECKLE SMOOTHING
5. TYPE OF REPORT & PERIOD COVERED: Technical Report
6. PERFORMING ORG. REPORT NUMBER

7. AUTHOR(s): (10) C. R. Christensen, B. D. Guenther, J. S. Bennett and Nicholas George
8. CONTRACT OR GRANT NUMBER(s): (16)

9. PERFORMING ORGANIZATION NAME AND ADDRESS
Commander
US Army Missile Research and Development Command
ATTN: DRSMI-RR
Redstone Arsenal, Alabama 35809

10. PROGRAM ELEMENT, PROJECT, TASK AREA & WORK UNIT NUMBERS
(DA) 1W362303A214
AMCMS Code 632303.11.21414

11. CONTROLLING OFFICE NAME AND ADDRESS
Commander
US Army Missile Research and Development Command
ATTN: DRSMI-TI
Redstone Arsenal, Alabama 35809

(11)

12. REPORT DATE: 19 Jul 76
13. NUMBER OF PAGES: 53

14. MONITORING AGENCY NAME & ADDRESS (if different from Controlling Office)
(12) 54p.

15. SECURITY CLASS (of this report): UNCLASSIFIED
15a. DECLASSIFICATION/DOWNGRADING SCHEDULE

16 DISTRIBUTION STATEMENT (of this Report)

Approved for public release; distribution umlimited.

(14) DRDMI-TR-RR-77-2

17 DISTRIBUTION STATEMENT (of the abstract entered in Block 20, if different from Report)

18. SUPPLEMENTARY NOTES

19. KEY WORDS (Continue on reverse side if necessary and identify by block number)

20. ABSTRACT (Continue on reverse side if necessary and identify by block number)

A theory is presented which relates the minimum detectable contrast level for an object in the presence of noise to the statistics of the speckle. Consideration is given to smoothing of the noise by multiple looks and by area. Measurements of the minimum detectable contrast are made for two types of speckle noise. First, a coherent, plane wave is added to an ideal diffuse wave and the threshold of detection is established as a function of the beam ratio.
(Continued)

DD FORM 1 JAN 73 1473 EDITION OF 1 NOV 65 IS OBSOLETE

UNCLASSIFIED 40 211 AB
SECURITY CLASSIFICATION OF THIS PAGE (When Data Entered)

20. ABSTRACT (Continued)

Second, these results are compared to the technique of speckle smoothing using an N-fold intensity superposition of fully developed speckle pattens. Good agreement of experiments with theory is observed. The equivalence of four different methods of N-look averaging is shown and it is demonstrated that fully developed speckle leads to an image degradation independent of light level over a very wide range of light levels. Detection probabilities and false alarm probabilities are determined from observations on random arrays of high-and low-contrast discs.

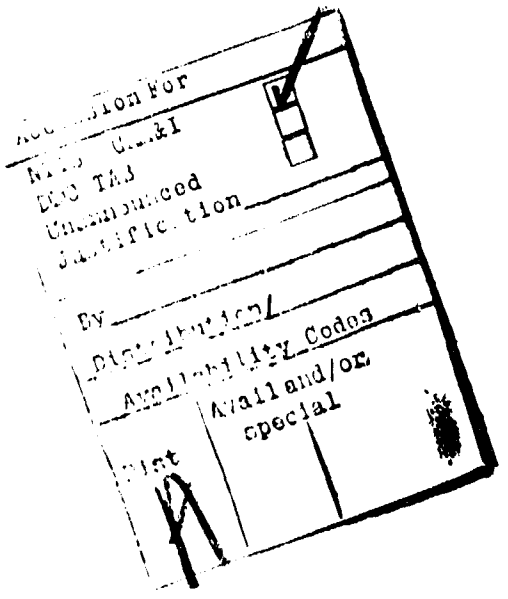

CONTENTS

ILLUSTRATIONS

ILLUSTRATIONS (Concluded)

ACKNOWLEDGMENTS

The assistance of R. R. Lattanzi in generating the random disc arrays is gratefully acknowledged.

1. INTRODUCTION

In monochromatic illumination, objects whose roughness is on the order of a wavelength or so cause speckle to appear in the reflected signal. This phenomenon is well known, as it has been studied extensively during the past 15 years. While much interest has centered on speckle in optical processing, imaging, holography, and in particular on the suppression or smoothing of speckle, there is growing interest in the study of speckle in images from illumination by monochromatic sources lying outside the visible band. Speckle noise occurs in the display of microwave radar images, where it is better known as scintillation. It is also prevalent in spatially scanned systems operating from the submillimeter to the visible region.

Numerous recent treatments of multiple-look smoothing of speckle noise are described in the review by McKechnie.[1] However, it is difficult to compare them because sufficient data on the initial distribution of the intensity have not been included or a highly nonlinear film-recording process has been used to record the multiple-look sequence. Hence, there has not been much accord as to the number of looks which one should design into a display to achieve a given resolution and quality in the final imagery.

In studies of speckle smoothing, either opaque discs or highly contrasted binary images, such as resolution charts, have been employed.[2] Other recent studies have included the use of realistic imagery; but in these, it is difficult to make a quantitative determination of the contrast levels involved.[3] Since in practical applications imagery of low contrast is often encountered and since speckle noise is particularly severe at low contrasts, this specific problem merits careful study.

In this study our objective is to provide new data on the detection of low-contrast objects in speckled imagery and to present the data in a form which is general enough that it can be easily applied to any wavelength or band of interest. The study of three different types of aperture smoothing and the presentation of illumination level tests for fully developed speckle are reported. Detection probabilities and false-alarm rates for objects in speckle noise are discussed and the results of experiments are shown.

While the presentation of thresholds of detectable contrast is emphasized, e.g., in

---

1. T. S. McKechnie, "Speckle Reduction," *Laser Speckle*, J. C. Dainty, ed., Springer-Verlag, Berlin, 1975, p. 123.

2. J. C. Dainty, "Detection of Images Immersed in Speckle Noise," *Optical Acta*, Vol. 18, 1971, pp. 327-339.

3. A. Kozma and C. R. Christensen, "The Effects of Speckle on Resolution," *Journal of the Optical Society of America*, Vol. 66, 1976, pp. 1257-1260.

Figures 10 and *12*, the original photographs are reported in enough detail so that one can independently establish results on other important questions that are beyond the scope of this report. An illustration of the latter is a count of false-alarm rates for various sizes of low-contrast images.

An excellent account of detection theory applied to the problem of detecting small images immersed in a background of laser-produced speckle is given by Dainty.[3] The density functions for some important cases of monochromatic illumination that has been speckled are given by Goodman.[4]

This consideration is limited to a study of the two main types of speckle noise which are likely to be encountered in laser and microwave ranging systems. However, the speckle noise is described in general terms, abstracted away from any specific system, so it is hoped that the results will be generally applicable for system design. Specifically, the following two classes of speckle noise are considered: one arises from the superposition by intensity of N-independent fully developed speckle patterns, and the second occurs with the coherent superposition of a diffuse (fully developed speckle) beam and a plane wave beam.

An expression is derived for the minimum detectable gray level which is observable as a function of the speckle noise present in the imagery. In a practical system the origin of the speckle which we treat is due to the reflection of a monochromatic wave by some diffuse object, including the convolving effect of the input scanning or other effective aperture. While considerable interfacing is required in the usual system for this input speckle noise to manifest itself as noise in the display, we circumvent this specialization by means of a simple laser analog experimental configuration. This is shown in *Figure 1* and is described in detail in a later section of this report.

In our research the study of speckle noise as it influences contrast detectability is new. With an adaptation of Rose's test chart,[5] we study threshold limits of discernible contrast as the statistical parameters of the illumination are varied. The transmission chart is composed of an array of circular densities varying in transmissivity along one axis and in diameter along the other, as shown in *Figure 2*. Having various densities and areas on a single chart greatly facilitates the recording of speckle images, since the numerous inevitable fluctuations then occur simultaneously to all data.

---

4. J. W. Goodman, "Statistical Properties of Laser Speckle Patterns," *Laser Speckle*, J. C. Dainty, ed., Springer-Verlag, Berlin, p. 9.

5. Albert Rose, *Vision, Human and Electronic*, Plenum Press, New York, 1974.

Study of smoothing by area and measurement of contrast levels follows readily from this chart, as is detailed below in the explanation of *Figures 6* through *9*.

For images in speckle, detection or resolution can be expected to improve if independent intensity patterns, or looks, are superimposed. This is well known and is readily explained based on the fact that the fluctuation σ_u in the mean value of the sum of N-independent terms is smaller than the rms value of a single term σ_1. The smoothed value for the standard deviation is $\sigma_u = \sigma_1 / N^{1/2}$.

The same basic notion is applicable to image area. Hence, if an image has a gray area which encompasses many speckles, there is a tendency for a viewer to average over the intensity fluctuations. In brief, larger areas of low contrast are more likely to be detected than smaller ones. This improvement should be related to the number of independent looks, areawise, given by A/s^2, where A is the area of constant gray level and s is the lineal dimension of a speckle in the image.

Thus, the parameter $\sigma_u s/[<u>A^{1/2}]$ is proposed as a criterion for minimum detectable contrast, as given in Equation (11), where σ_u is the rms fluctuation in the illumination at the image and $<u>$ is the mean value of this intensity. Using this notion we consider the equivalence, insofar as discernible contrast, between sources having equal values for this ratio. While a good understanding of the variation in the threshold of detection with illumination statistics is obtained using this ratio, one should consider it as an approximate guideline. Two factors prevent a rigorous interpretation. One is that with differing density functions and nonadditive noise, actual explicit calculations of quantities such as detection probability, false-alarm rate, etc., proceed in a more fundamental way simply by using the more complete statistical functions. Signal-to-noise characterizations can lead to inconsistencies.[2] The second is that human observers are used to establish the detection thresholds, and there are many subtleties in perception which have never been characterized algebraically.

The results on minimum detectable contrast at various areas give useful data against which one can test various hypotheses about averaging and correlation trends in human vision. These are beyond the scope of the present report.

2. SPECKLED IMAGES

While speckle-degraded imagery occurs in a wide variety of radar systems from microwave to optical and including the newer submillimeter systems, the specific sources of the imagery are not discussed in this section. Here we consider a transmission mask T(x,y) which has simple circular disc patterns. This is illuminated by monochromatic laser light and the speckle is introduced in a controlled way using a

diffuser in the illuminating light. The object transparency is imaged, as shown in *Figure 1*, through a pinhole or small aperture which has the effect of increasing the speckle size so that it can be photographically recorded and studied with relative ease independently of film grain size. In the theory below, it is shown how speckle noise and its smoothing in complex imaging systems can be directly related to our results using a simple transmission chart and controlled laser illumination.

Consider the one-dimensional transmission function shown in *Figure 3*. The relatively clear background is shown by T_2 with a step decrease in transmission to T_1, for the length interval X. The incident illumination intensity is denoted by u(x). A simple imaging lens system is used to give the final speckled image. The light intensity I(x) recorded as signal at an arbitrary position x is given by

$$I(x) = T_1 u(x). \tag{1}$$

The fluctuation in u(x) caused either by source unevenness or the interference phenomenon known as speckle is characterized by a density function f(u). The size of the speckle in the output plane is controlled by the aperture size D, being approximately given by $(\lambda/D)L$, where λ is the illumination wavelength and L is the distance from the second lens to the image recording plane. A second-order density function $f(u_1, u_2)$ is necessary to describe these spatial characteristics in detail. However, here we need only to know how many speckles occur per unit area and how to compute the smoothed variance in a sample mean from the single element variance σ_1 and the number of independent samples N (i.e., by $\sigma^2 = \sigma_1^2/N$). Hence, in the analysis herein, a knowledge of the first-order density f(u) will suffice. For interesting specific problems where a knowledge of second-order densities or correlation functions is useful in the study of imaged speckle, the reader is referred to the literature.[1,2,4,6]

For the intensity u and its density f(u), the usual notation is summarized below for the mean, mean-square, variance, and characteristic function, respectively:

$$\langle u \rangle = \int_{-\infty}^{\infty} u f(u)\, du, \tag{2}$$

$$\langle u^2 \rangle = \int_{-\infty}^{\infty} u^2 f(u)\, du, \tag{3}$$

$$\sigma_u^2 = \langle u^2 \rangle - \langle u \rangle^2, \tag{4}$$

$$F(\eta) = \int_{-\infty}^{\infty} f(u)\, e^{i\eta u}\, du. \tag{5}$$

In the image intensity given by Equation (1), there is a noise or fluctuation in intensity σ_1, as follows:

---

6. N. George and A. Jain, "Space and Wavelength Independence of Speckle Intensity," *Applied Physics*, Vol. 4, 1974, pp. 201-212

$$\sigma_1 = T_1\sigma_u. \tag{6}$$

To detect the change in signal which results from a step in transmission, T_2 to T_1, the following inequality should be met:

$$(T_2 - T_1)u \geq \tfrac{1}{2}\sigma_u(T_1 + T_2). \tag{7}$$

To include the effect of threshold-setting criteria of various types, let O_m denote the observer's signal-to-noise factor. Then in consideration of false-alarm rates, if tangential signal levels are set or if observer-to-observer variability is to be studied, these effects are lumped into O_m, and Equation (7) becomes

$$(T_1 - T_2)u = O_m\sigma_u T_{12}, \tag{8}$$

where the average transmission value is denoted by $T_{12} = \frac{1}{2}(T_1 + T_2)$.

While Equation (8) is written for point detection, it is clear in looking at an image of our version of Rose's test chart, *Figure 2*, that an observer visually averages over the disc area A which contains a number of fluctuations in intensity u. If the shape is intricate, undoubtedly the observer's processing is complex. For convenience in analysis, we consider the following simple model. Let the observer-model perceive the intensity given by the sample mean of u. For a speckle length s and an area A, over which the transmission is fixed at T_1, there are N *independent* samples given by

$$N = (A/s^2)M, \tag{9}$$

M is the number of looks arising as independent speckle patterns are superimposed. These are independent if different diffusers are used, i.e., different members from an ensemble. Uncorrelated speckle patterns can also be obtained by moving the controlling pupil if it is translated in its plane by one or more diameters D.

The assertion that the number of independent samples over the area A is given by dividing A by the average area of a speckle, i.e., approximately s^2, is an entirely separate matter. If by s, one means the characteristic length determined by the spatial fall-off of the second-order correlation function, then there is no ambiguity. However, if one takes $s = (\lambda D)L$, then the following physical argument is appropriate. In image plane speckle, intensity fluctuations corresponding to speckles arise from the diffuser properties mapped to the image plane on a resolution-by-resolution cell basis. Hence, for a diffuser close to the object itself with the fine scale roughness of opal glass, the diffuser's roughness has a correlation length which is much smaller than the size of a resolution cell referenced to the object plane, and the speckle size in the output plane is almost entirely controlled by the resolution cell. Thus, in the image plane the pattern is decorrelated on a speckle-to-speckle basis, just as one would surmise from a casual visual observation. This topic is discussed more fully elsewhere.[6]

Averaging over the area A, and using Equations (8) and (9), we can write the detection criterion for the gray scale change $T_2 - T_1$ as follows:

$$(T_2 - T_1)\langle u\rangle A \geq \frac{O_{sn}\sigma_u T_{12} A}{[(A/s^2)M]^{1/2}} . \qquad (10)$$

In an exact analysis of detector smoothing, Goodman[4] has calculated a factor $\mathfrak{M}$, which can be substituted into Equation (10) for more accuracy, i.e., $\mathfrak{M}^{1/2} = \langle u\rangle A^{1/2}/(\sigma_u s)$.

With Equation (10) one can consider a variety of problems. If there is nonlinear processing, then the total signal given by $(T_2-T_1)\ \langle u\rangle A$ should be used in the argument of the function which describes the processing. This is the rationale for including the A on both sides of Equation (10). Again, in the problem of calculating the minimum number of photons required to enable one to see slight changes in object contrast, given by $(T_2-T_1)/T_{12}$, one uses the total number of photons from A. For white light if the total number of photons associated with $\langle u\rangle$ T_1A is n_o, then the variance term $\sigma_u T_1 A$ is $(n_o)^{1/2}$. In detecting images with the ratio $\sigma_u/\langle u\rangle = 1/(n_o)^{1/2}$, several interesting consequences are described by Rose.[5] Neither of the problems described above is treated further in this report.

Herein we consider systems operating at high flux levels using monochromatic light. For this situation the ratio of $\sigma_u/\langle u\rangle$ is established by a consideration of the interference phenomenon alone. Hence, Equation (10) is rewritten in terms of detectable contrast in the image $(T_2-T_1)/T_{12}$ as it relates to the "effective contrast" in the source illumination denoted by the ratio $\sigma_u/\langle u\rangle$. The resulting expression is

$$\frac{T_2 - T_1}{T_{12}} \geq O_{sn}\frac{\sigma_u}{\langle u\rangle} \times \frac{1}{(AM/s^2)^{1/2}} . \qquad (11)$$

3. STATISTICS OF THE ILLUMINATION IN THE IMAGE PLANE

In order to have data on threshold detection for a wide variety of systems, it is important to use a variety of source configurations. The many specific systems used in optical processing, ranging, scanning, and holography are too numerous and varied to permit any sort of exhaustive listing. Just listing systems of interest in speckle smoothing takes several pages of textual description to explain.[1]

Our approach is to specify the density function and the contrast ratio of the illumination referenced to the output plane in the absence of a test object. While only one type of nonscanned, fully illuminated object is considered, the results will be applicable to any system having the same statistics in the illumination at the image.

In this context one should note that object roughness controls the degree to which speckle develops. And, of course,

object reflectivity in comparison to the surroundings defines a gray level or object contrast. Scanning spot size or transmitter and receiver beam sizes control the speckle dimension. Thus, in an attempt to encompass a variety of systems, we study the detection of low-contrast objects for several different density functions of image illumination.

It is interesting to study the minimum levels of contrast which can be detected in objects as a function of the different types of noise. From Equation (11) it is concluded that as long as the spot size A and the speckle size s are unchanged, one needs only to specify the ratio $\sigma_u/\langle u\rangle$ for the source illumination in order to calculate the detectable contrast level. As $\sigma_u/\langle u\rangle$ increases the detection is degraded. As is well known for fully developed speckle, this contrast ratio is unity; and the detectable $(T_2-T_1)/T_{12}$ is poor, i.e., high. Also, it is level independent. Hence, increases in intensity $\langle u\rangle$ do not improve this situation at all. This is contrary to our experience in the white light case for which, as explained above, the ratio $\sigma_u/\langle u\rangle$ decreases as the root of the intensity of illumination (see *Table 1*). Fortunately, with monochromatic illumination there are many techniques by which speckle can be minimized and also many situations in which the speckle initially is not fully developed. Nevertheless, it remains as a possible serious degradation factor; and it is important to understand in basic terms so that it can be minimized or smoothed in an efficient way.

The statistical properties of the illumination in the image plane are reviewed below.[4,6-9]

A. FULLY DEVELOPED SPECKLE

In this case the plane wave beam in *Figure 1* is blocked and the test pattern is illuminated using the argon laser-opal glass diffuser with polarization analyzer as shown in *Figure 1* to eliminate any cross-polarized component which may occur.

For speckle in the image plane of the test pattern with the basic configuration shown in *Figure 1* and with R = 0, the electric field at any position is a complex-valued random walk. With an opal glass diffuser the number of independent fluctuations in phase per resolution cell, referenced to the object plane, is large. It is further asserted that the opal glass is thick enough or the diffuser is rough enough, to give an rms-

7. J. M. Burch, "Interferometry with Scattered Light," in *Optical Instruments and Techniques*, J. Home Dickson, ed., Oriel, Newcastle upon Tyne, England, 1970.

8. J. D. Briers, "A Note on the Statistics of Laser Speckle Patterns," *Optical Quantum Electronics*, 1975, pp. 422-424.

9. A. Papoulis, *Probability, Random Variables, and Stochastic Processes*, McGraw-Hill Book Company, New York, 1965.

deviation in phase much larger than π-radians. The scalar component of electric field in the image plane has a well-known statistical description.[1,2,5,7] From the central limit theorem it follows that the density function for the electric field is Gaussian. The real and imaginary components of this complex-valued field are normal, independent random variables with zero means. The probability density function for the absolute value of this field is the Rayleigh density. From this, it follows that the density f(u) for the intensity u is given by the damped exponential:

$$f(u) = (e^{-u/a}/a)H(u), \tag{12}$$

where H(u) is the unit step

$$H(u) = \begin{cases} 1, & u \geq 0, \\ 0, & u < 0. \end{cases} \tag{13}$$

The density, average value of intensity $\langle u \rangle$, variance σ_u^2, and contrast ratio C_R are given in *Table 1*.

B. SUPERPOSITION OF N-FOLD SPECKLE INTENSITIES

A very important method for smoothing speckle is simply to combine independent intensity patterns linearly. If photographs are recorded as different diffusers are inserted, then one approaches this result. In this case the sample mean u is defined as follows:

$$u = (1/N)(u_1 + u_2 + \cdots + u_N). \tag{14}$$

Asserting that the u_k are independent then by Equations (5) and (14), we have the characteristic function for u given by the product of the characteristic functions for the u_k, as follows:

$$\langle \exp(i\eta u) \rangle = \langle \exp(i\eta u_1/N) \rangle \cdots \langle \exp(i\eta u_N/N) \rangle. \tag{15}$$

From Equation (12), the density function for the kth component is

$$f(u_k) = (e^{-u_k/a}/a)H(u); \tag{16}$$

and by Equation (15), the appropriate Fourier transform $F_k(\eta/N)$ is given by

$$F_k\left(\frac{\eta}{N}\right) = \int_{-\infty}^{\infty} f(u_k)\, e^{i\eta u_k/N} H(u_k)\, du_k,$$
$$F_k(\eta/N) = (1 - i\eta a/N)^{-1}. \tag{17}$$

Since the transforms in Equation (17) are all equal, the N-fold product which is the characteristic function for the density of u is given by

$$F(\eta) = [(1 - i\eta a/N)^{-1}]^N. \tag{18}$$

This is inverted using Equation (3.382.7) of Gradshteyn and Ryzhik[10] to obtain

$$f(u) = [(Nu)^{N-1} e^{-Nu/a}/a^N(N-1)!]H(u). \tag{19}$$

From the basic definitions and using Equation (3.381.4) of Reference 10, one can

10. I. S. Gradshteyn and I. M. Ryzhik, *Tables of Integrals, Series, and Products*, Academic Press, New York, 1965.

obtain any order of moment $\langle u^m \rangle$. For the mean, mean square, and variance, respectively, we find the following expressions:

$$\langle u \rangle = a, \quad \langle u^2 \rangle = (1 + 1/N)a^2, \quad \sigma^2 = a^2/N. \quad (20)$$

These results are also presented in *Table 1*. Comparing the contrast ratios for white light and for this case of N-fold superposition, we note that there is a direct analogy between variation of photon flux in white light and the number of independent looks for fully developed speckle. This correspondence is borne out as is seen if one compares threshold-detection photographs at low intensities in white light[5] to the data presented in Sections 5 through 7.

C. FULLY DEVELOPED SPECKLE BEAM ADDED TO A MONOCHROMATIC PLANE WAVE

Several authors have treated the problem of calculating the density function for the intensity when a diffuse beam is interferometrically added to a monochromatic plane wave.[4] Careful measurements of the intensity resulting when a laser beam is transmitted through opal glass of varying thicknesses show excellent agreement with the theoretical density functions for this case.[11] In the experiments reported in this paper, the configuration used is ideal. The thick opal glass diffuser creates a fully developed speckle pattern, and the use of a completely separate channel for the interferometric addition assures us of a precisely known beam ratio parameter R. In this case the density function is given by

$$f(u) = \exp[-(u + u_0)/u_s]\, I_0[2(u\, u_0)^{1/2}/u_s]\, H(u)/u_s, \quad (21)$$

where u_o is the intensity of the plane wave reference and u_s is the average intensity of the fully developed speckle component measured in the image plane. The function I_o is the modified Bessel function of order zero. The beam ratio R, defined in Equation (22), is a highly controllable easily measured parameter. R is given by

$$R = u_0/u_s. \quad (22)$$

D. BEAM RATIO AND THE NUMBER OF LOOKS

From Equation (11), the minimum detectable contrast $(T_2\text{-}T_1)/T_{12}$, is proportional to the ratio $C_R = \sigma_u/\langle u \rangle$. Hence, from *Table 1*, it is expected that *approximately* the same degradation should result in the minimum detectable gray level in case (ii) or (iii) if one equates their respective C_R parameters, as follows:

$$1/N^{1/2} = (1 + 2R)^{1/2}/(1 + R). \quad (23)$$

11. N. George, A. Jain, and R. D. S. Melville, "Experiments on the Space and Wavelength Dependence of Speckle," *Applied Physics*, Vol. 7, 1975, pp. 157-169.

Solving for R in terms of N gives the following equivalence:

$$R = N - 1 + [N(N-1)]^{1/2}, \quad R \approx 2N - \tfrac{1}{2}. \qquad (24)$$

It should be emphasized that the density functions in these cases need *not* be equal. In fact, for *small* values of N the density function in Equation (19) is not even close to that in Equation (21) for the corresponding beam ratio R given by Equation (24). However, since the noise fluctuation is characterized by the rms deviation σ_u, if two distinct noise sources have equal ratios of $\sigma_u/\langle u \rangle$, then one should anticipate approximately equal limits in detectable contrast. This is an interesting conjecture since the configurations used to obtain these two distributions are generally quite different. Also in some practical systems, it may be meaningful only to obtain speckle smoothing by an N-fold superposition, whereas in the laboratory simulation it is much easier to add coherently a controlled level of plane wave reference.

4. THE EXPERIMENTAL SETUP

In order to establish the criteria for design of coherent imaging systems that will encounter low-contrast objects, the laser analog experimental configuration shown in *Figure 1* was used. This setup, which employs an adaptation of a test pattern developed by Rose[5] as an object, offers a simple and convenient means to evaluate threshold limits of discernible contrast as the statistical parameters of the illumination are varied. The effect of speckle noise in the imagery, as it influences contrast detectability, may be studied in a controlled manner by the use of a diffuser in the illuminating light and a variable-size aperture in the imaging system.

The transmission test pattern, shown in *Figure 2*, consists of a Cartesian array of circular discs varied in transmission along the x axis but of fixed radius; while along the y axis it is varied in radius by factors of two at fixed density. The actual transmissions and diameters obtained in the mask are shown in *Figure 2*. For the experiments reported in this report, two test patterns containing different ranges of density were constructed by illuminating 649F glass plates with white light through a step wedge and a set of holes drilled in a thin metal plate. The glass plates were then developed in POTA developer to give a γ of 0.9. (POTA is composed of 1-phenyl-3-pyrazolidone, 1.5 g; sodium sulfite, 30 g; and cold water (25° C) to make 1000 cm^3.) Subsequently, the sensitizing dye was removed from the plates by immersing them into a 30% solution of pyridine. The actual measured transmission factors, T_1, and disc diameters used in the experiments are listed in *Figure 2*. Plate 1 was used in the experiments unless noted otherwise.

Each transmission test pattern was installed in the object position of the optical system shown in *Figure 1* and illuminated

with light from an argon-ion laser operating at 0.488 μm. Initially, the laser beam was divided into two parts whose intensities could be controlled independently to any desired level by variable attenuators. Each beam was then expanded and collimated. Speckle with controlled polarization was produced in one of the beams by means of a Kodak 500 μm thick opal glass diffuser followed by an analyzer to select one polarization component. Subsequently, the two beams were added coherently at a beam splitter as shown in *Figure 1* and used to illuminate the test pattern. The collimated plane wave beam was blocked in experiments requiring only diffuse illumination.

The transmitted signal was recorded on Polaroid film using a telescope with unity magnification consisting of two 629-mm focal length f/5 lenses; L_1 and L_2 in *Figure 1*. Imaging through a sufficiently small aperture had the effect of increasing the speckle size so that it could be photographically recorded and studied with relative ease independent of film grain size. Apertures of 200-, 400-, and 600-μm diameter have been used in these experiments. The 600-μm aperture produced speckle in the imagery approximately equal in size to the smallest (0.88-mm diameter) disc in the test target and was used in all experiments unless otherwise noted.

The linear speckle dimension, $s = \lambda f/D$, where f is the focal length of lens L_2 and D is the aperture diameter, was 0.5 mm when the 600-μm diameter aperture was used. For all images recorded and displayed in this report, the film exposures were adjusted to stay within the linear portion of the film response.

5. ILLUMINATION LEVEL AND IMAGE QUALITY

With reference to *Table 1*, it is noted that the white light image improves greatly as the light level increases. This is well known, and commonly with degraded or noisy images the first remedial action is to increase the illumination from the source. For monochromatic illumination with N-looks it is seen from Case II.2. of *Table 1* that the role of N in decreasing the illumination contrast ratio is analogous to the role of the photon flux, n_o, with white light. Thus, to a large extent, research results in which white light is used can be expected to have this direct analogy in the case of monochromatic illumination, i.e., photon flux in the white light case acts in direct analogy to the number of independent looks using monochromatic illumination. In this context the experiments in white light shown in *Figures 1.6* and *2.6* of Rose[5] show a striking similarity, as regards both detection and image quality, to data presented here in which monochromatic light is used.

Using this analog we would expect the N = 1 case, termed fully developed speckle, to result in very badly degraded images. Of

course, the analogy is not essential in this case since the contrast ratio of unity corresponds to a signal-to-noise ratio of unity. This is known *a priori* to yield poor image quality.

But now notice that the contrast ratio $C_R = 1$ is computed without regard to the illumination level of the laser. Does this mean that the image quality is independent of brightness once the illumination is above the thermal fluctuation level? The answer is yes, and this is shown in *Figure 4* where an *exposure range* of 16:1 is used. Almost no difference is observed in which of the gray discs are seen as the exposure is increased from E = 1 to 16 (relative units).

While this result is not new, photographs demonstrating this effect have not been found in the published literature. Of course, one must keep the illumination above the photon flux noise and below the saturation levels of the film, and in *Figure 3* the E = 1 value is too low. A common misconception in laboratory technique with speckled imagery is to find the "optimum" exposure level with meticulous care to record data over the entire dynamic range of the film. From *Figure 4*, it is clear that a better procedure is to expose for the mid-range of the film since no amount of darkroom artistry is going to provide good image quality when speckle illumination is degrading the imagery.

6. EXPERIMENTS WITH VARYING SPECKLE SIZE

As noted in the Introduction, in the perception of a disc of constant gray level in speckled imagery of our version of Rose's test pattern, *Figure 2*, an observer visually averages over the intensity fluctuations due to speckle encompassed by the disc area. If the shape is intricate, undoubtedly the observer's processing is complex. For convenience in analysis, however, consider the following simple model. Let the observer perceive the sample mean of the intensity μ. We assert that, for disc area A and average lineal speckle dimension s in the image plane, the visual averaging process is equivalent to taking N independent samples given by $N = A/s^2$. The assertion that the number of independent samples over the disc area is given by dividing A by the average area of a speckle, i.e., approximately s^2, requires that the speckle pattern be decorrelated on a speckle-to-speckle basis. A detailed discussion of this point is found in Reference 8. Goodman[4] obtains a similar result when evaluating speckle smoothing by a finite detector aperture. While our approach is not analytically precise, it can be used to estimate the smoothed variance in a sample mean of the intensity, σ, using the single element variance σ_1 and the number of independent samples, N, from $\sigma = \sigma_1/(N)^{1/2} = \sigma_1 s/A^{1/2}$. Thus the fluctuation in the mean

value of μ perceived by the observer is smoothed by an amount which depends on the relative size of the disc and the speckle. From this simple argument we conclude that for low-contrast images in speckle, the visual detection process should be expected to improve as the image area increases or the speckle size decreases.

In order to study this notion experimentally, three sets of images of test pattern, Plate 2, *Figure 2*, were recorded with each set having different speckle size. The speckle size was controlled by adjusting the diameter of the aperture in the imaging system shown in *Figure 1*. The 600-, 400-, and 200-μm apertures used for the set of images shown in *Figure 5* produced speckle in the imagery having lineal dimension, $s = \lambda f / D$, of 0.5, 0.75, and 1.5 mm, respectively. The images shown in the first row of *Figure 5* were recorded without speckle and indicate the system resolution with each aperture. Note that with the 200-μm aperture in place, the smallest (0.88-mm diameter) disc in the test pattern is not well resolved. The striations visible in these images are due to inhomogeneities in the emulsion of the test pattern.

The set of images displayed in the second row of *Figure 5* show the effect of speckle size on the visual detection process. Columns 4 through 8 of test pattern, plate 2, are shown. It is noted that with the 600-μm aperture, rows 1 and 2 of the test pattern are detected reliably. The row 2 diameter is 7 times the speckle size while row 3, which is detected with some difficulty, is a factor of 3.5 times the speckle size. As the speckle size is increased to 1.5 mm in column 3 of *Figure 5*, both rows 3 and 2 of the test pattern disappear while row 1 remains easily visible. The disc diameter in row 2 of the test pattern is 2.4 times the speckle size while row 1 is 4.7 times the speckle size. Clearly, for a given speckle size, the larger the area of the disc, the easier it is to detect it in the image. These observations are in good agreement with the prediction by Dainty (top-hat or high-contrast case) of 95% detection probability for an image diameter of four times the speckle size.[2]

The images displayed in *Figure 5* show the improvement in detectability achieved from speckle smoothing by superposition of independent speckle patterns in the manner discussed in Section 7.

7. COMPARISON OF MULTIPLE LOOK METHODS FOR SMOOTHING

A. INTENSITY SUPERPOSITION OF N LOOKS

For the addition of speckle patterns on an intensity basis with the plane wave reference absent, $R = 0$, three separate methods were used. While they are by no means identical, under controlled conditions, they were found to give essentially equivalent results with regard to minimum detectable object contrast, speckle contrast, and image appearance.

B. N-SEPARATE OPAL GLASS DIFFUSERS USED

In the ensemble of N-diffusers method, a different opal glass diffuser was used to produce the speckle field for each exposure. Images of test pattern, plate 1, Columns 1-7, formed by multiple exposure recording for N = 1, 2, 4, 8, 16 independent speckle patterns are shown in *Figure 6*. The array of discs illuminated is four rows by seven columns. With reference to *Figure 2*, the transmission values run from 0.88 to 0.047. The most dense column (0.018) has not been illuminated. Note that row 4, for which the disc diameter is about equal to a speckle size, is not detected at all in the one-look case due to the high false-alarm rate. In the original photographic data two or perhaps three of the row-4 discs are seen but only when N = 16. It is clear that one can read, quantitatively, the variation of threshold contrast as a function of N for a fixed size of disc. Average data of this type from several observers are included in *Figure 10*.

In the event that printing has changed the resolution, some of the above discussion may have been confusing. However, the larger discs should be printed more legibly. Thus, centering attention on the largest discs, one should see all but the lowest contrast at N = 16, losing one by N = 4 and another at N = 1.

C. CASCADE OF TWO DIFFUSERS WITH MOTION

The cascaded diffusers technique involved placing a sheet of Kodak fine ground glass behind the opal glass diffuser and moving it between exposures. The diffusers are moved relatively slightly between the multiple exposures on film. This method has practical importance,[1,12,13] and so it is interesting to compare to the ensemble-average method described above. To obtain good decorrelation of speckle, care must be taken to insure that neither diffuser has a specular component or hot spot. If it does, then in moving only one diffuser, some residual correlation exists and a more complex analysis is required to derive the statistics.[4] With imperfect diffusers the general case which needs to be analyzed is that in which N-fold partially correlated patterns are superimposed together with a plane wave reference.

Another subtle departure occurs if the temporal coherence length of the laser is relatively low, e.g., an etalon for single moding is not used. Then the diffuser cascade will give speckle of lowered contrast

---

12. S. Lowenthal and D. Joyeux, "Speckle Removal by a Slowly Moving Diffuser Associated with a Motionless Diffuser," *Journal of the Optical Society of America*, Vol. 61, 1971, pp. 847-851.

13. E. G. Rawson, A. B. Nafarrate, R. E. Norton, and J. W. Goodman, "Speckle-free Rear-Projection Screen Using Two Close Screens with Slow Relative Motion," *Journal of the Optical Society of America*, Vol. 66, 1976, pp. 1290-1294.

due to the larger path differentials which occur, i.e., light reaching a given point on the opal glass comes from many points on the ground glass, travels for significantly different path distances, and results in a partial loss of coherence in the illuminating beam.

Nevertheless, if suitable care is taken, data for N-fold superpositions are essentially indistinguishable from that shown in *Figure 6*. *Figure 7* shows the results of superimposing up to 128 images formed using different positions of the cascaded diffusers. Columns 1-7 of test pattern, plate 1, are shown.

D. N-POSITIONS OF THE CONTROLLING PUPIL

In the third method for obtaining independent speckle patterns the aperture shown in *Figure 1* was moved a distance equal to several times its diameter between exposures. Due to convenience this method was used to obtain the data on resolution and detectable contrast for multiple looks presented in the following sections.

To make the speckle size large enough so that film grain effects are unimportant and so that the speckle is comparable to the smallest disc size, a small pupil is used (*Figure 1*). Moving the pupil in the plane by its own diameter (or by a few diameters) is adequate to decorrelate the speckle. First we discuss the N-fold averaging using this method and second, we present data showing averaging over a range of N from 1 to 128.

An any point in the image plane, the electric field can be written as a summation over a small resolution cell centered at the corresponding point in the object plane. With the unity magnification in the system shown in *Figure 1*, a pupil size D gives a speckle size s and an impulse response w on the order of $w \approx s \approx \lambda F/D$, where F is the focal length. How much should we move the pupil? A mathematical answer is given by Equation (4.9) of Reference 1. Herein, we present a simple physical description.

Consider the field emanating from only a single resolution cell in the object. The transverse correlation length of this radiation as it crosses the plane of the pupil is on the order of $\lambda F/w \approx D$; but of course, it is the pupil size! Thus, moving the pupil by several times D gives rise to a spatially random selection of brights and darks for the particular image point. Since the same portion of the opal glass diffuser gives rise to the entire N-fold intensity samples at its corresponding image position, it is reasonable to think of this as a spatial sampling of the far-field speckle pattern due to the diffuser of size w. Thus, in establishing experimentally that the pupil motion leads to a smoothing which is essentially equal to that for the ensemble average, we provide a direct verification of the applicability of the ergodic hypothesis to this problem.

Test photographs for this method are shown on the left-hand side of *Figure 8*. Images of the test pattern, plate 1, were formed by multiple exposures on Polaroid film in the image plane of *Figure 1*. Only diffuse illumination was used; the uniform plane wave beam was blocked. A 600-μm telescope aperture was used in the imaging system and was displaced 2 mm between exposures to produce independent speckle patterns. The exposure times were adjusted to correspond to the linear part of the film response curve. This facilitates reading data from the photographs, although the detectability is independent of exposure value. Index markers, 1-8, in the figure refer to the test chart column numbers in *Figure 2*. The N superimposed images of the test chart shown in the left-hand columns of *Figure 8* can be seen to give equivalent results to those for methods one and two shown in *Figures 4* and *5*. Data from the photographs in *Figure 8* were used to plot the curves in *Figure 10*.

8. MULTIPLE LOOKS BY POLARIZATION DIVERSITY

It has previously been shown that thick opal glass diffusers, such as the 500-μm diffusers used in these experiments, produce nearly complete depolarization of the transmitted light and the perpendicular components of polarization yield uncorrelated speckle fields.[14] Therefore an image of the test pattern illuminated by the diffuser is equivalent to a superposition of two images with independent speckle patterns. This equivalence is demonstrated in *Figure 9*. Columns 1-6 of the test pattern are shown. *Figure 9b* shows a multiple exposure formed by moving the aperture in *Figure 1* between exposures to produce independent speckle patterns. An analyzer was placed after the diffuser, as shown in *Figure 1*, to allow only the vertical component of polarization to illuminate the test pattern. To form the image shown in *Figure 9a* the analyzer was removed producing two uncorrelated speckle patterns for each position of the aperture. In this case only four exposures were required to produce eight independent superimposed patterns. It is seen that the minimum detectable contrast for each row is the same in *Figures 9a* and *9b* demonstrating the validity of using polarization diversity for speckle averaging. In all cases in which multiple superpositions of speckle fields were made, the analyzer was removed to reduce the number of exposures required by factor of two.

9. MULTIPLE LOOKS AND THE SPECULAR BEAM RATIO

The effect on image detectability of N-fold superpositions of independent speckle patterns is shown in the left-hand side of

14. N. George, A. Jain, and R. D. S. Melville, Jr., "Speckle, Diffusers, and Depolarization," *Applied Physics*, Vol. 6, 1975, p. 65.

Figure 8. The lowest density disc detectable in each row of the test pattern was determined for each value of N and the results from observations by several individuals were averaged. The object contrast ratios are shown in *Figure 10*; T_1 is the transmission of the disc and T_2 is the transmission of the background. The object contrast is $(T_2-T_1)/T_{12}$, where $T_{12} = \frac{1}{2}(T_1 + T_2)$. The points at $N = \infty$ were obtained by continuously moving a ground glass diffuser behind an opal glass diffuser during the exposure and correspond to the noncoherent case.

For equal illumination contrast ratios, C_R, obtained by different speckle smoothing techniques, the minimum detectable object contrast ratios $(T_2-T_1)/T_{12}$, should be approximately equal. From the expressions for C_R in *Table 1* the illumination contrast ratios are found to be equal for speckle averaging by superposition of N independent speckle fields and for the addition of a speckle beam to a plane wave reference beam when

$$R = N - 1 + \sqrt{N(N-1)} \quad . \qquad (25)$$

The right-hand side of *Figure 8* shows images recorded when the test pattern was illuminated with the plane wave coherently added to the diffuse beam at the beam splitter shown in *Figure 1*. Their electric field vectors are collinear. The ratios of plane wave to diffuse beam intensity $R\ u_o/u_s$ used in recording the images were calculated from Equation (25), using the values of N in the left-half of *Figure 8*. The index lines labeled 1-8 are to identify positions on the transmission mask reading from right to left in *Figure 2*. Separate photographs were taken for each R value in order to include the full range of disc transmittances and also to provide an independent photograph with some data overlap. Images covering a greater range at R-values are shown in *Figure 11*.

The threshold level of detectable contrast is plotted versus the beam ratio in *Figure 12*. These data were obtained from *Figure 8*, using several observers who were instructed to decide whether or not they detected a disc. These curves should be viewed as preliminary since numerous human factors which are important in such testing were largely ignored. For example, there is a considerable difference between the threshold of detection and object recognition, and it was clear during the testing that this caused some spread in the data.

It is seen by comparing the images in *Figure 8* that the object detectabilities and speckle contrasts are approximately the same for the N-look images and the speckle beam plus plane wave beam images. The measured deviation from equivalence of the minimum detectable object contrast for the two methods of illumination is shown in *Figure 13*. This plot illustrates that slightly lower contrast discs are detectable in the

two-beam method than for the equivalent [by Equation (2)] N-looks. This is expected from the lower speckle field contrasts for the mixed beam imagery seen in *Figure 8*.

Figures 10 and *12* are examples of how one might use the experimental technique to obtain design parameters for a coherent imaging system. From *Figure 10* we see that if the speckle size is equal to the object size we must detect, then 4-looks must be made before an object with maximum contrast can be observed. The same data however shows that we can trade resolution for minimum detectable contrast, i.e., by reducing our resolution requirement by a factor of four we can observe a minimum detectable contrast of 0.9 with 4-looks.

The data shown in *Figure 12* can be used in the same way to evaluate system performance. For example, if the diffuse component reflected from an object is 10% of the specular reflection, then we can determine the minimum detectable contrast at different resolutions for R = 10.

10. PROBABILITIES OF DETECTION, FALSE ALARMS AND MISSED SIGNALS

The regular spacing of the test pattern used in determining minimum detectable contrast conveys a strong clue to the observer. This probability somewhat squelches the false alarm and missed signal rates and invalidates its use for testing these aspects. A transmission test target consisting of a random array of discs was therefore designed. A random two-dimensional array of points, such as that shown in *Figure 14*, was generated and plotted by a computer. This was used to construct an array of discs, all of the same diameter and contrast. This array was used as the input to the optical system in *Figure 1* and a set of images recorded for different values of N, R or speckle size.

Observers were shown a disc of the same contrast and size as those in the test pattern and asked to locate all similar discs in the images. Probabilities for detection, P_D, missed signals, P_M, and false alarms, P_F, were defined as

$$P_D = \frac{n_o}{n}$$

$$P_M = \frac{n-n_o}{n} = 1 - P_D$$

$$P_F = \frac{n_F}{n} \qquad (26)$$

where n is the total number of discs in the test pattern, n_o is the number correctly located, and n_f is the number the observers thought they saw which were not on the test pattern.

Images of 1.77-mm-diameter high contrast discs, $(T_2-T_1)/T_{12} = 1.97$, are shown in *Figure 15* for values of N up to N = 8. The probabilities from observations by a group of individuals are plotted in *Figure 16*. From *Figure 10*, a minimum detectable contrast of

1.97 for a 1.77-mm-diameter disc corresponds to N = 1. In *Figure 16* at N = 1, the detection probability is 50%, indicating that the knowledge of disc location in the regular array increased the observer signal-to-noise factor, as would be expected.

The detection process by observers can be modeled as a search over the image for areas of known size having average density values lying within a defined range or window. In detecting the high-contrast discs, the observer is required to set only the upper density threshold defining this window; the lower value is effectively zero due to the limited dynamic range of the image recording medium. *Figure 17*[7] displays the intensity probability density, $p(u)$ when no signal is present. For small values of u, $p(u)$ decreases with N, yielding a correspondingly rapid increase in detection probability and decrease in false-alarm probability. For high-contrast targets, i.e., when target u is much less than $\langle u \rangle$ a discussion of single threshold machine detection of high-contrast discs has been given by Dainty[7] and the results may be qualitatively applicable to this simplified visual model.

Images of 1.77-mm-diameter discs with contrast, $(I_2-I_1)/I_2$ of 0.23 are shown in *Figure 18* and the detection probabilities and false-alarm probabilities plotted as a function of N in *Figure 19*. For the detection of low-contrast discs the observers have the difficult task of defining both upper and lower density thresholds and applying them consistently over a large variation in speckle noise contrast. Human factors, such as training, therefore become more important than for high-contrast disc detection and may explain the lack of close agreement between the detection probabilities in *Figure 19* and the minimum detectable contrast for row 3 in *Figure 10*.

If the signal u_1 has an intensity near $\langle u \rangle$, i.e. a low-contrast signal, then from *Figure 17* the probability density at u_1 increases with N at small values of N, then approaches zero as N becomes large. The probability of finding a false signal with the intensity u_1 is given by $p(u_1)$. With a detection window around u_1, the false-alarm rate should also reach a maximum value at intermediate values of N. From an examination of *Figure 18*, the maximum in P_1 can be seen to lie at approximately N = 8 for this low-contrast disc. Although this was observed by some of the individuals whose readings were averaged for *Figure 19*, the effect is masked by the large variance in P_1 for the observer group. The extremes for P_1 for the observers are from 0 to 1.8 at low values of N.

Figure 20 shows images of 0.233 contrast discs 1.77 mm in diameter at values of R equivalent to the N-values in *Figure 18*. The detection probabilities and false-alarm probabilities are plotted in *Figure 21*. The agreement with the N-look probabilities is within the observer error.

To avoid the experimental difficulties and uncertainty resulting from using human observers, future efforts will be directed

toward the use of machine detection to measure false-alarm rates and detection probabilities.

II. CONCLUSIONS

An expression is derived for the threshold object contrast that is detectable in the presence of speckle noise [see Equations (10) and (11)]. The effects of smoothing by area (trading resolution) and by multiple looks are included. A convenient characterization of the speckle noise is the ratio of rms fluctuation to average intensity, i.e., $\sigma / \langle u \rangle$.

While the idealized damped exponential density is commonly used in speckle studies, herein, we have used two more general cases (*Table 1*) which cover a wide range of practical situations. For the N-fold intensity superposition, the quantitative decrease in minimum detectable object contrast has been measured as a function of N for different object sizes. Similarly, for the reference beam plus speckle case, the improved detectability with larger beam ratios R has been measured. The observed slopes in *Figures 10* and *12* are in accordance with the theory. The main results of the research are contained in these data. In their application to varied systems, first, one must make an estimate of the statistical density function which characterizes the background speckle noise. If one finds good correspondence to the densities in *Table 1*, then our data are applicable to the problem of establishing thresholds of detection for the system being analyzed.

The display of detection thresholds as a function of object size and contrast has been greatly facilitated through the use of our adaptation of Rose's test pattern. Other factors such as polarization, illumination level, wavelength, and recording medium are also readily varied. In the present report photographic data are provided to illustrate the effectiveness of this method. As an illustrative example, three different methods of smoothing speckle were studied. A complex analytical solution to this problem, described by McKechnie, has shown these methods to provide approximately equal smoothing. In our experiments, which are simple and straightforward, it is relatively easy to demonstrate this result. Additionally, experiments showing that the speckle decorrelates with input polarization are described. Experiments are also described showing that fully developed speckle leads to an image degradation that is independent of light level over a very wide range.

Random arrays of discs were used to determine false-alarm rates and detection probabilities for both high-contrast and low-contrast targets. The results for high-contrast discs show good agreement, both with the theoretical predictions of Dainty[7] and with our experiments on minimum detectable contrast. Accurate quantitative

measurements by human observers are more difficult for low-contrast discs, and the results are highly dependent on observer training and experience.

REFERENCES

1. McKechnie, T. S., "Speckle Reduction," *Laser Speckle*, J. C. Dainty, ed., Springer-Verlag, Berlin, 1975, p. 123.

2. Dainty, J. C., "Detection of Images Immersed in Speckle Noise," *Optical Acta*, Vol. 18, 1971, pp. 327-339.

3. Kozma, A. and Christensen, C. R., "The Effects of Speckle on Resolution," *Journal of the Optical Society of America*, Vol. 66, 1976, pp. 1257-1260.

4. Goodman, J. W., "Statistical Properties of Laser Speckle Patterns," *Laser Speckle*, J. C. Dainty, ed., Springer-Verlag, Berlin, p. 9.

5. Rose, Albert, *Vision, Human and Electronic*, Plenum Press, New York, 1974.

6. George, N. and Jain, A., "Space and Wavelength Dependence of Speckle Intensity," *Applied Physics*, Vol. 4, 1974, pp. 201-212.

7. Burch, J. M., "Interferometry with Scattered Light," in *Optical Instruments and Techniques*, J. Home Dickson, ed., Oriel, Newcastle upon Tyne, England, 1970.

8. Briers, J. D. "A Note on the Statistics of Laser Speckle Patterns," *Optical Quantum Electronics*, 1975, pp. 422-424.

9. Papoulis, A., *Probability, Random Variables, and Stochastic Processes*, McGraw-Hill Book Company, New York, 1965.

10. Gradshteyn, I. S. and Ryzhik, I. M., *Tables of Integrals, Series, and Products*, Academic Press, New York, 1965.

11. George, N., Jain, A., and Melville, R.D.S., "Experiments on the Space and Wavelength Dependence of Speckles," *Applied Physics*, Vol. 7, 1975, pp. 157-169.

12. Lowenthal, S. and Joyeux, D., "Speckle Removal by a Slowly Moving Diffuser Associated with a Motionless Diffuser," *Journal of the Optical Society of America*, Vol. 61, 1971, pp. 847-851.

13. Rawson, E. G., Nafarrate, A. B., Norton, R. E., and Goodman, J. W., "Speckle-free Rear-projection Screen Using Two Close Screens with Slow Relative Motion, *Journal of the Optical Society of America*, Vol. 66, 1976, pp. 1290-1294.

14. George, N., Jain, A., and Melville, R.D.S., Jr., "Speckle, Diffusers, and Depolarization," *Applied Physics*, Vol. 6, 1975, p. 65.

TABLE 1. DENSITY FUNCTION AND CONTRAST RATIO FOR SPECKLED ILLUMINATION IN THE IMAGE PLANE. THE BRIGHTNESS LIMITED CASE IS INCLUDED FOR WHITE LIGHT. (Tabulation is for f(u) when u ≥ 0; f(u) = 0 when u < 0. η_0 is the number of photons crossing per unit area; μ_0 is the plane wave intensity; μ_s is the speckle beam, average intensity; and $R = \mu_0/\mu_s$.)

Case	$f(u)$	$\langle u \rangle$	σ_u^2	$C_R = \sigma_u / \langle u \rangle$
(I) White light	...	u_0	u_0	$\frac{1}{(\pi\eta_0)^{1/2}}$
(II) Monochromatic light				
(i) Fully developed speckle	$e^{-u/a}/a$	a	a^2	1
(ii) Superposition of N-fold independent speckle intensities	$(Na)^{N-1}e^{-Nu/a}a^N(N-1)!$	a	$\frac{a^2}{N}$	$\frac{1}{N^{1/2}}$
(iii) Fully developed speckle beam interferometrically added to a plane wave reference beam,	$\frac{\exp[-(u+u_0)/u_s]I_0[2(uu_0)^{1/2}/u_s]}{u_s}$	u_0+u_s	$u_s^2(1+2R)$	$\frac{(1+2R)^{1/2}}{1+R}$

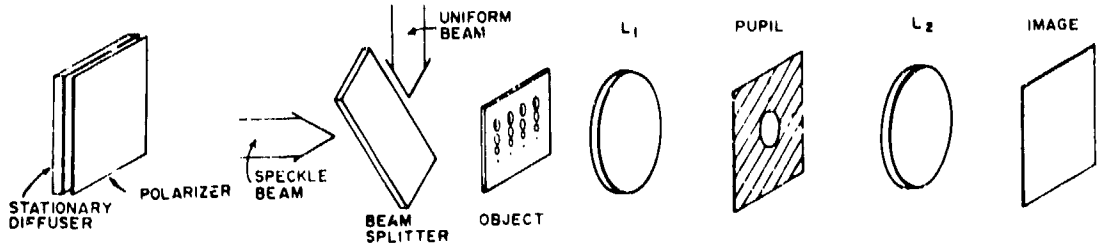

Figure 1. Setup for measuring thresholds of object contrast for speckled images. (The test object is imaged at unity magnification with a small pupil of diameter D to control the size of the speckle.)

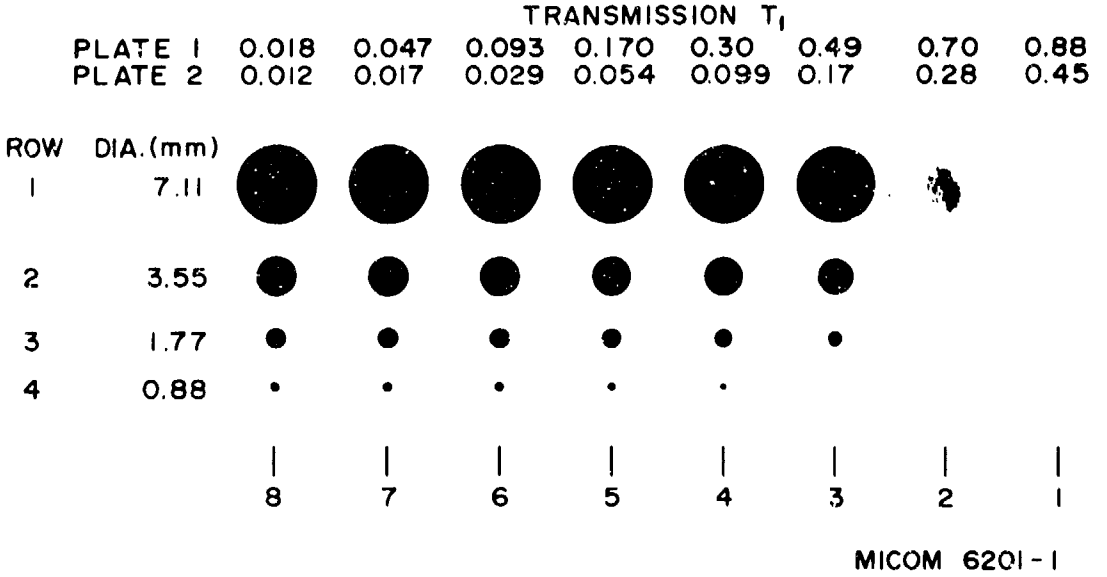

Figure 2. Test pattern. (The transmission for the two plates used in the experiments is shown at the top of the columns of discs. The integers at the bottom of each column and the row numbers are used in identifying discs in the text and other figures.)

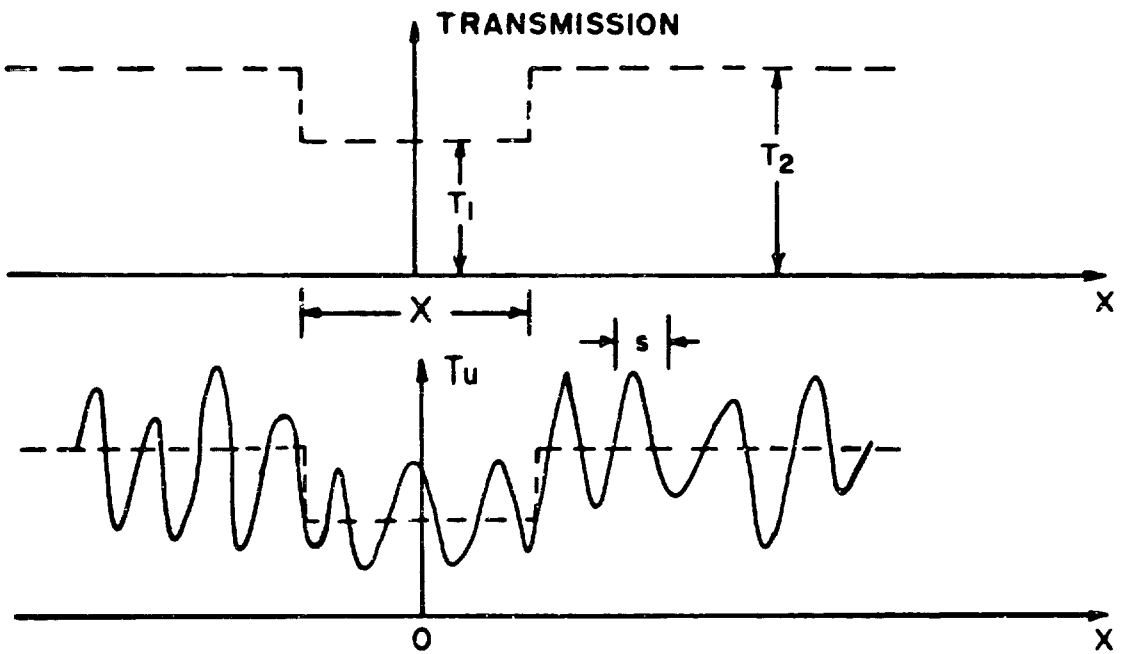

Figure 3. **Model for area averaging of speckle. (The signal T_1 is a dark spot in a bright background T_2 =1. The average length of a speckle is s and the signal extent is X).**

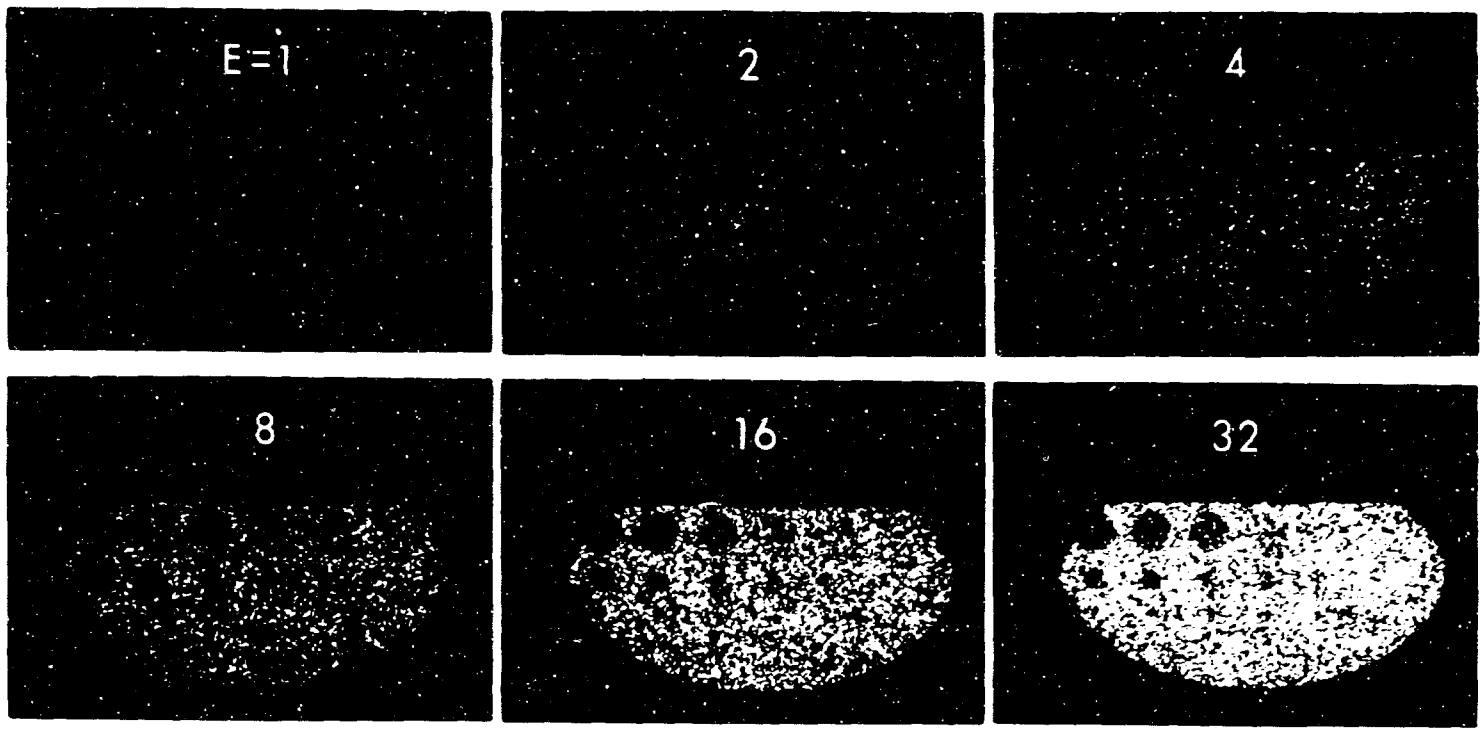

Figure 4. **Images of the same test pattern with diffuse illumination varying in relative intensity from 1 to 32. (Columns 1-6 of test pattern, plate 1, are shown.)**

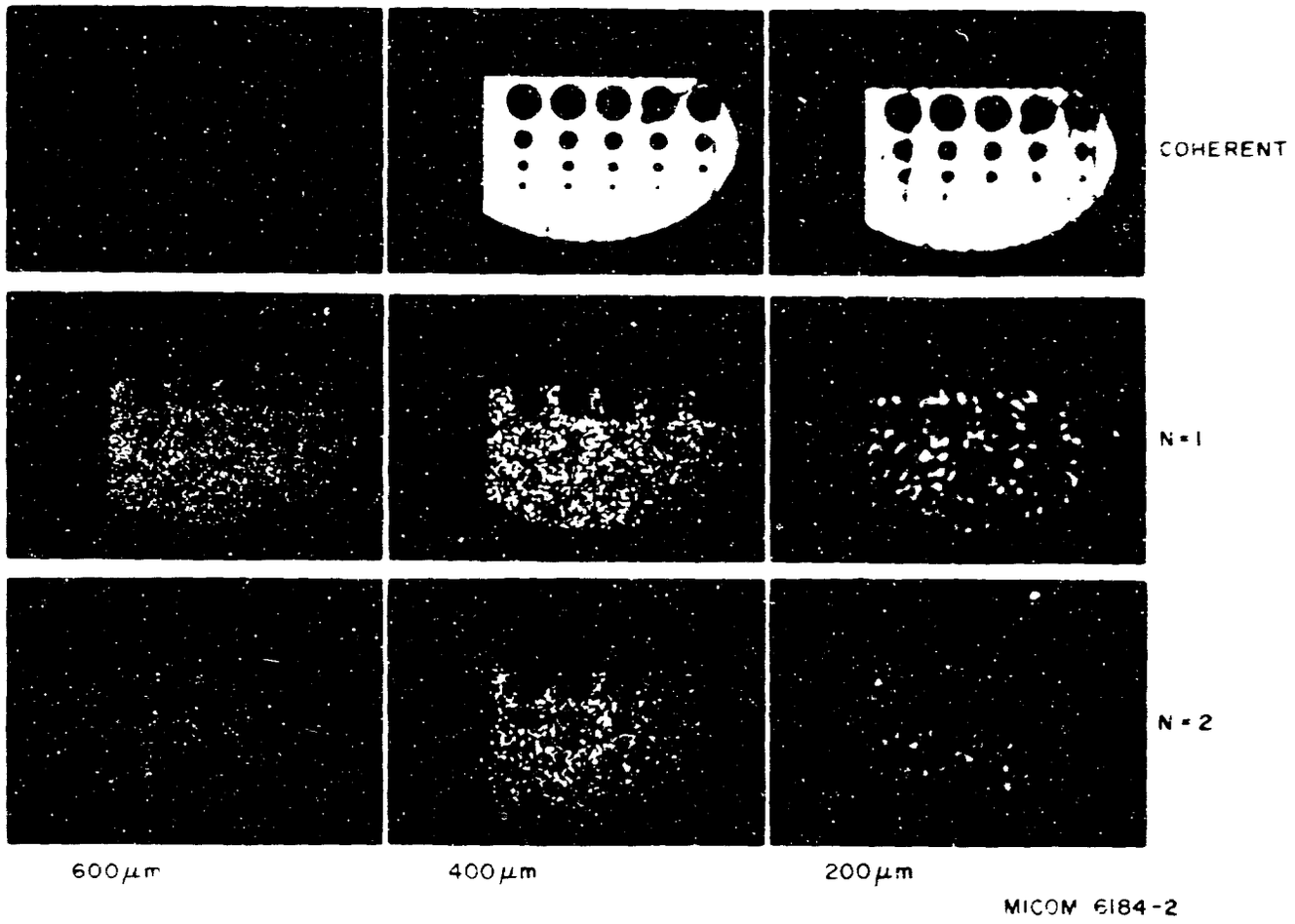

Figure 5. Effects of aperture size on resolution for coherent plane wave illumination and for illumination with one and two speckle fields. (Columns 4-6 of test plate 2 are shown.)

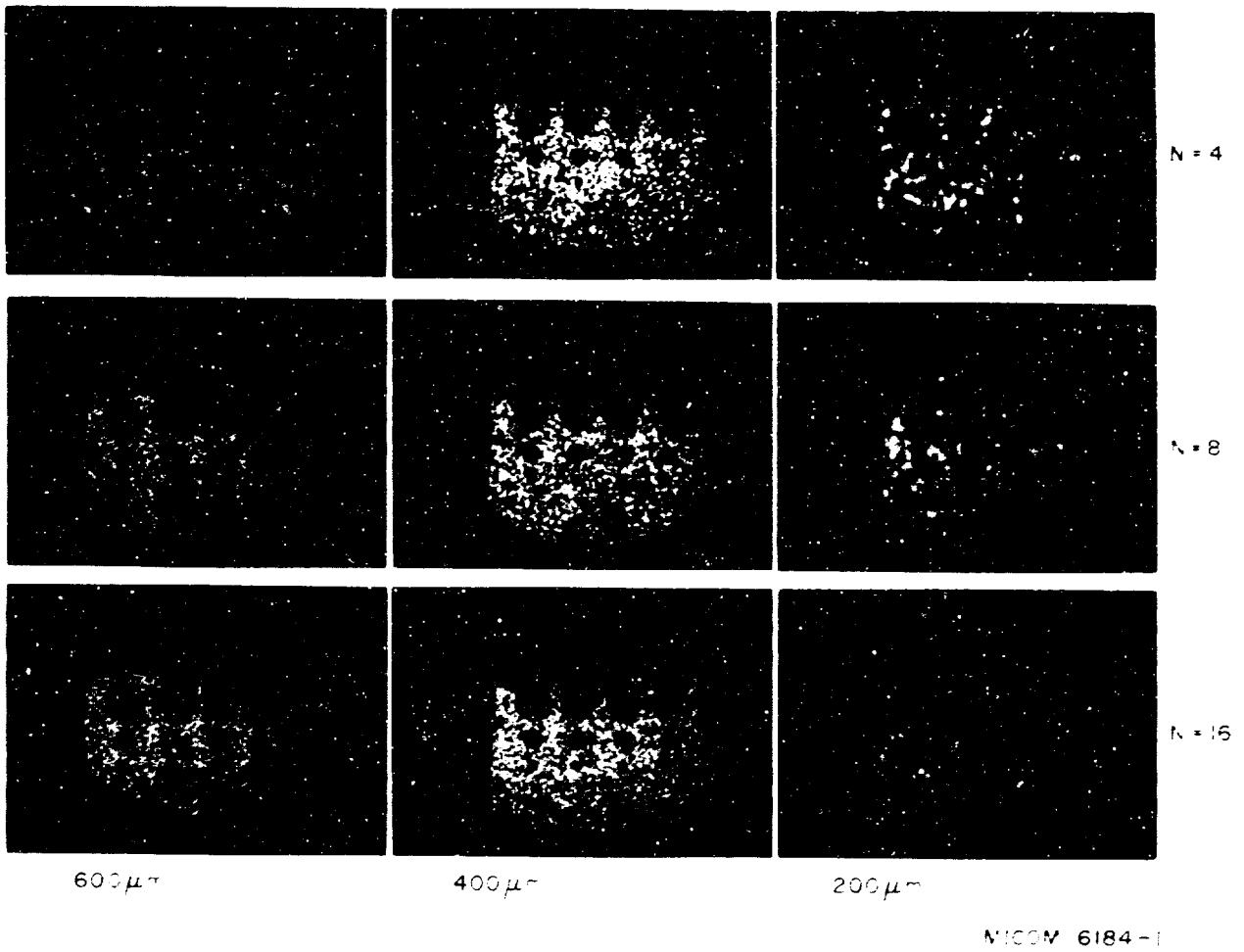

Figure 5. (Concluded)

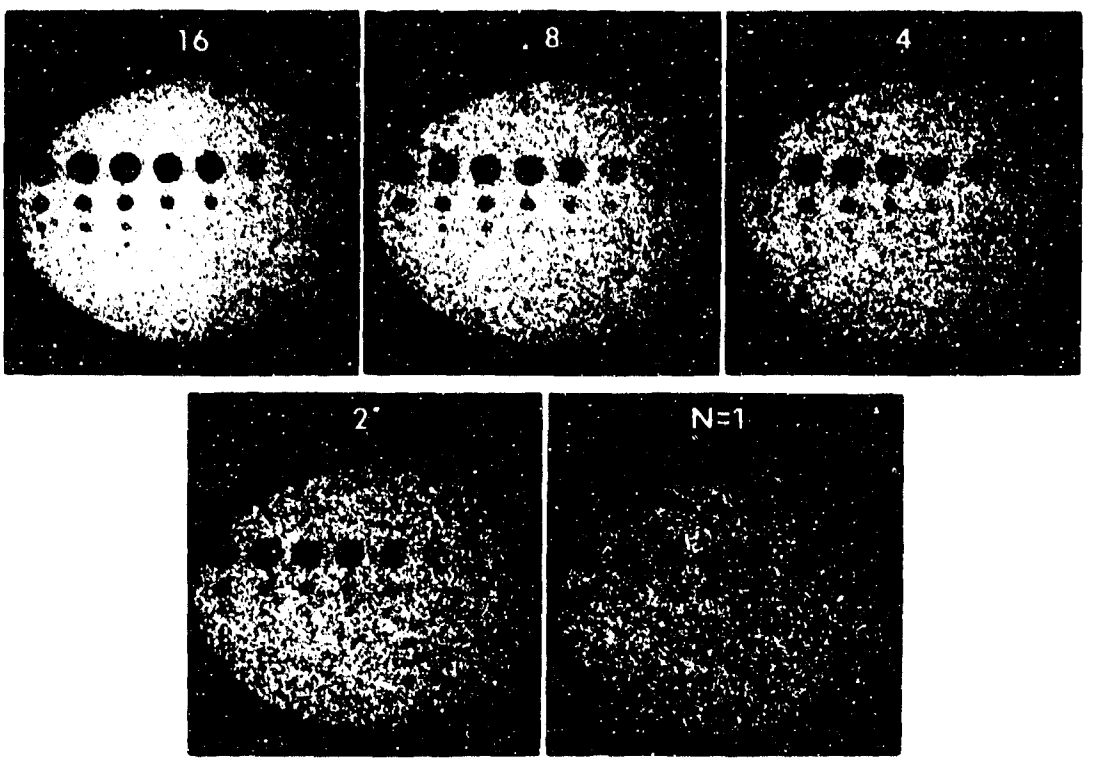

MICOM 6195-2

Figure 6. Speckle averaging by intensity superposition of speckle patterns from N different opal glass diffusers.

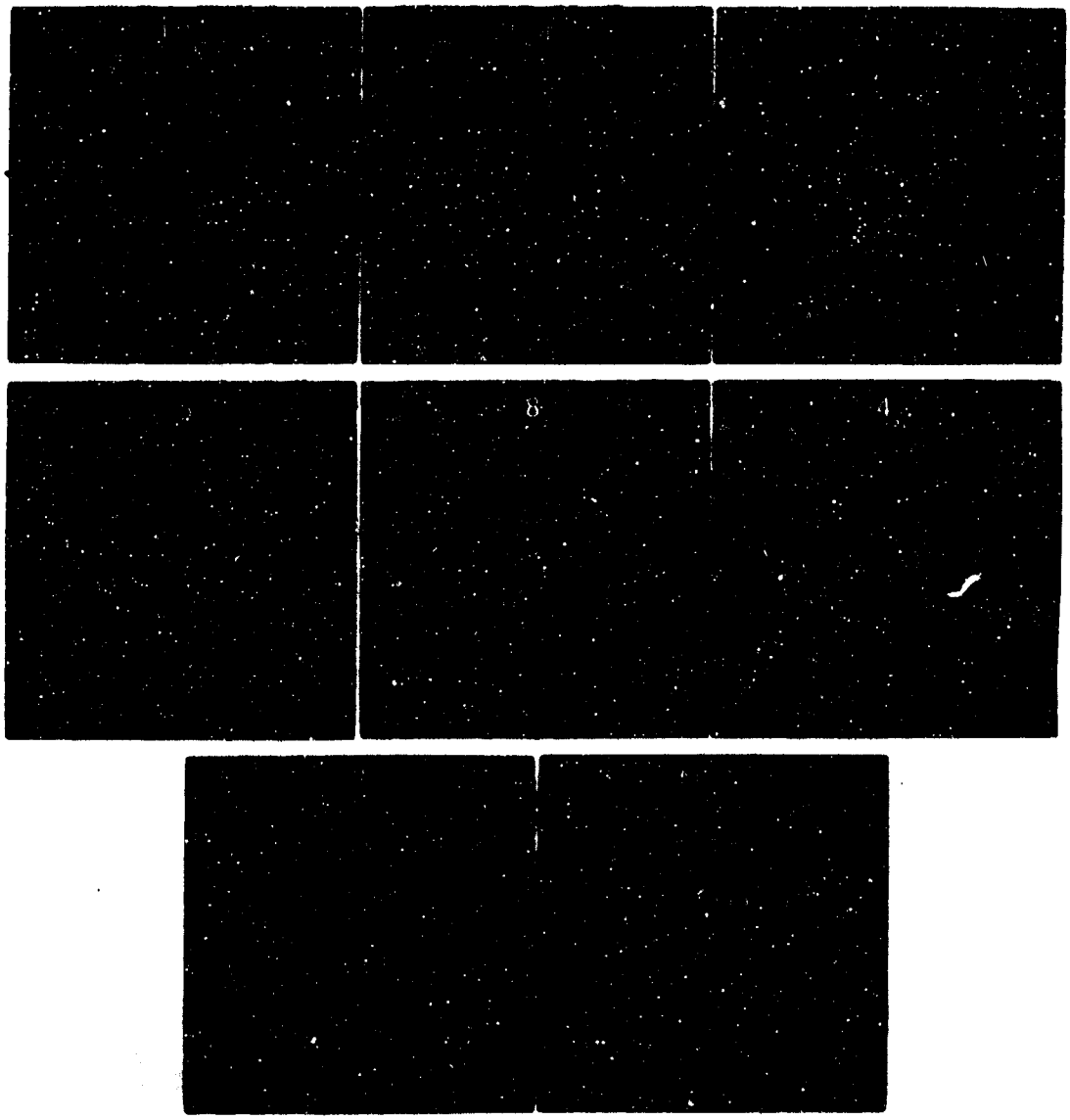

Figure 7. Speckle averaging by superimposing N speckle patterns from a cascaded ground glass and opal glass diffuser. (The first diffuser was displaced parallel to the second diffuser between exposures.)

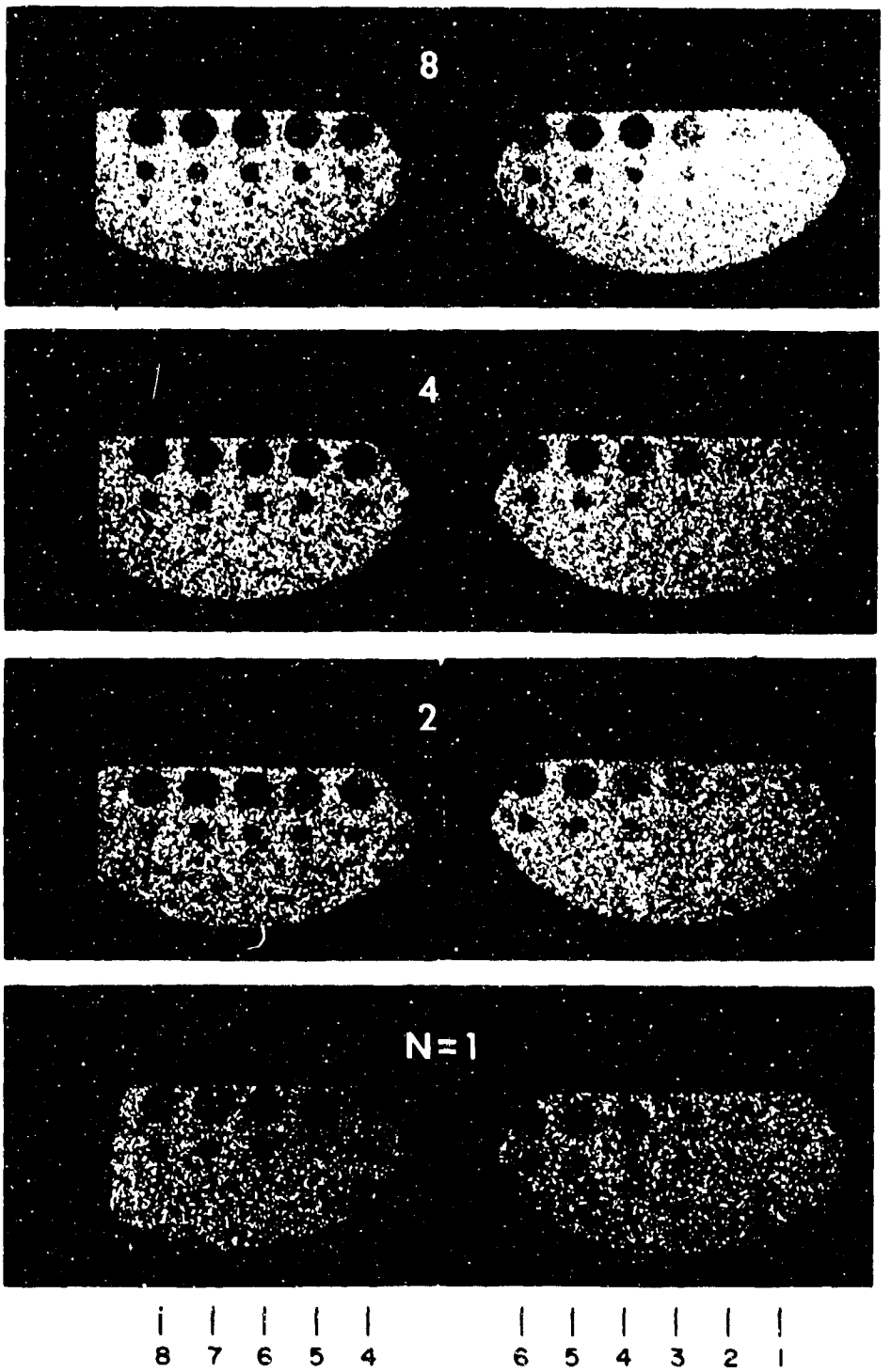

Figure 8. Comparison of test pattern images for N superpositions of independent speckle fields with images formed when the pattern is illuminated with a plane wave and a diffuse beam. [The ratios, R, of

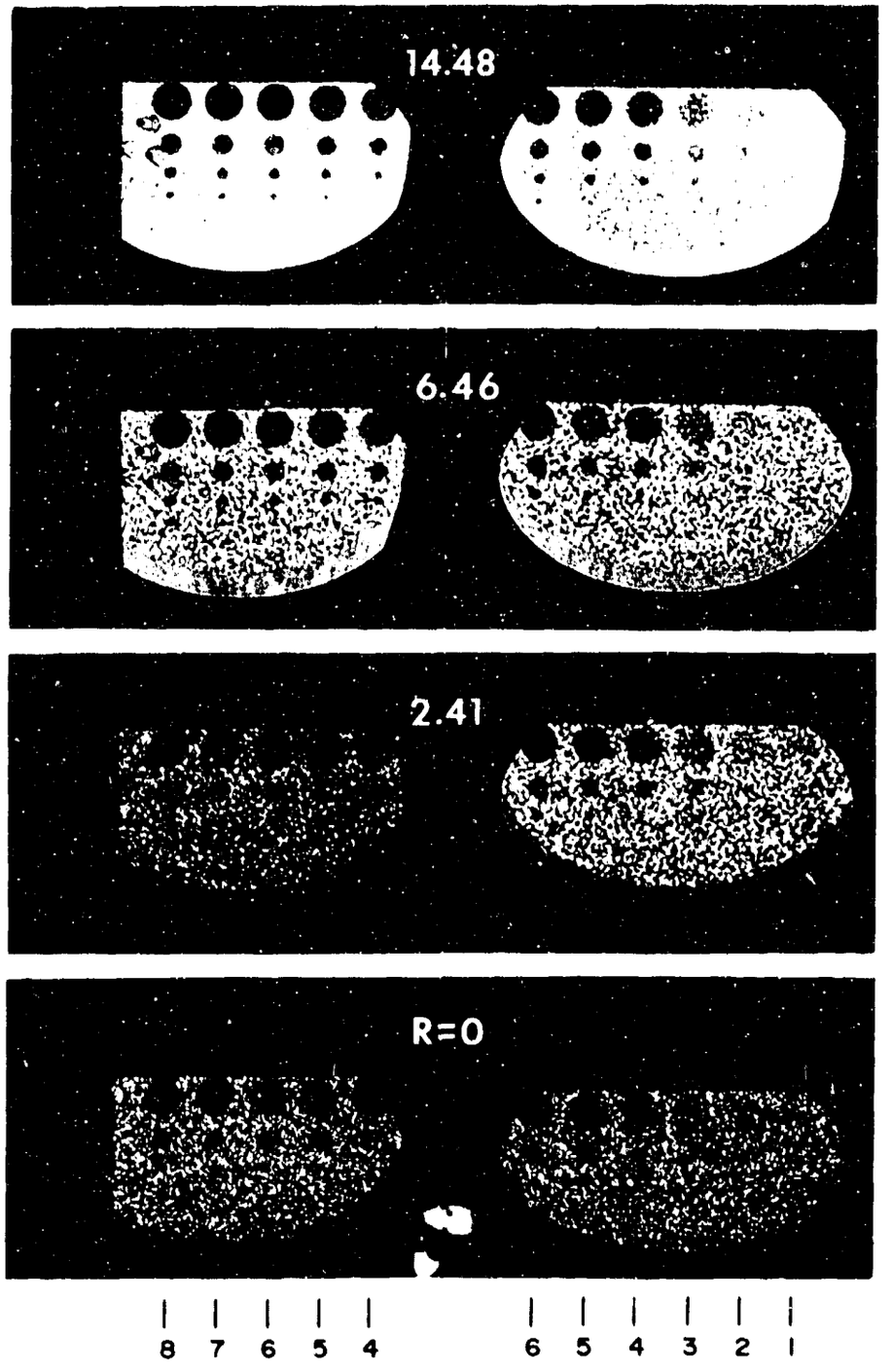

plane wave intensity to diffuse beam intensity chosen are equivalent by Equation (2) to the values of N for the adjacent images.]

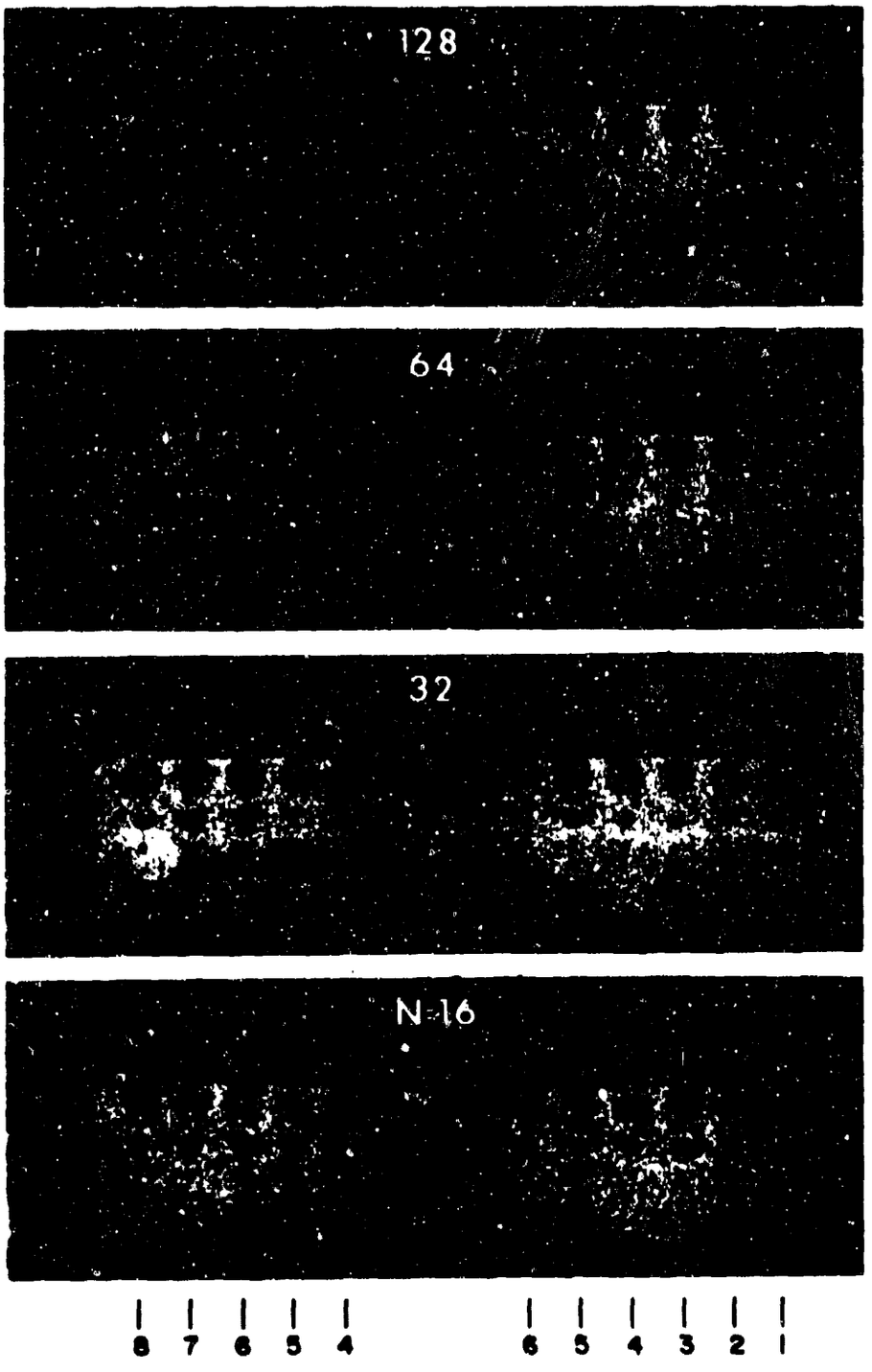
128
64
32
N-16
8 7 6 5 4
6 5 4 3 2 1

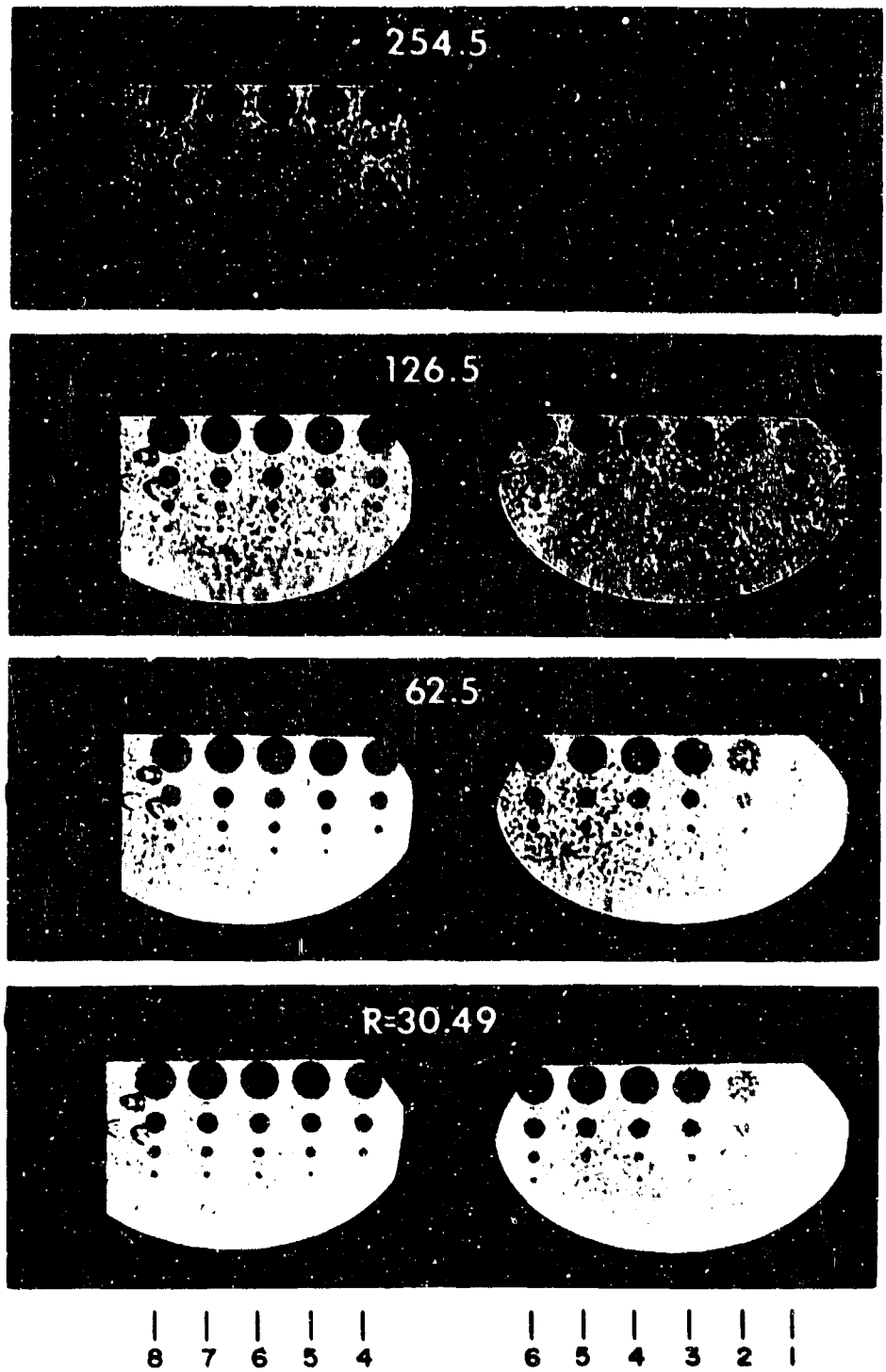

Figure 8. (Concluded)

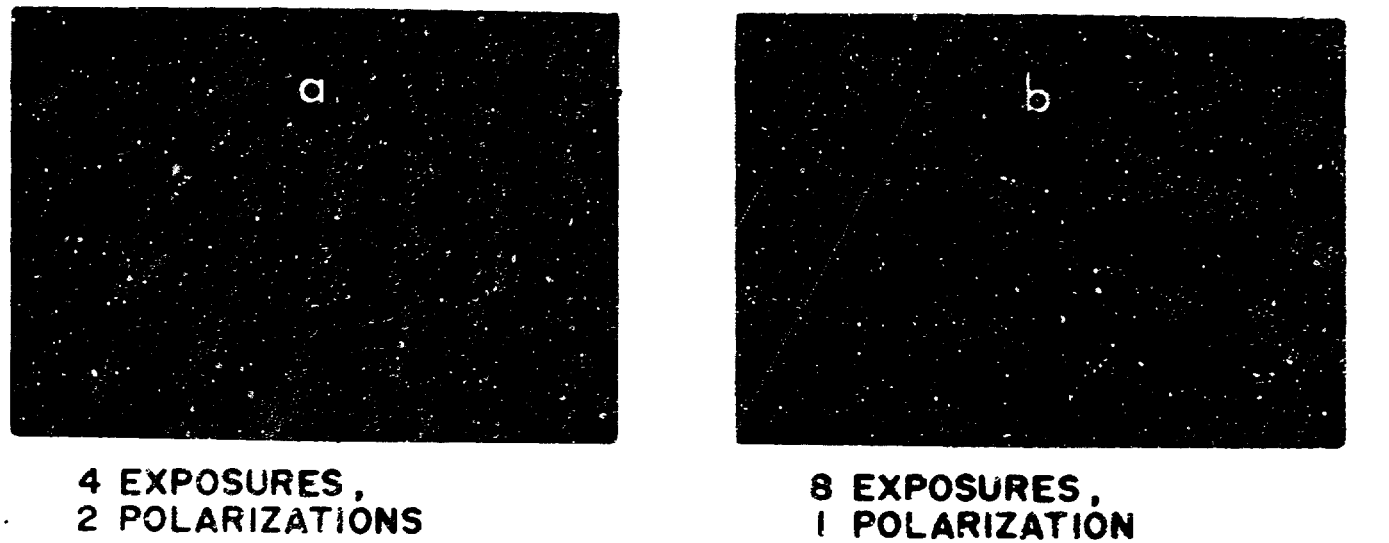

Figure 9. Comparison of speckle averaging by polarization diversity with averaging by displacement of the imaging system aperture.

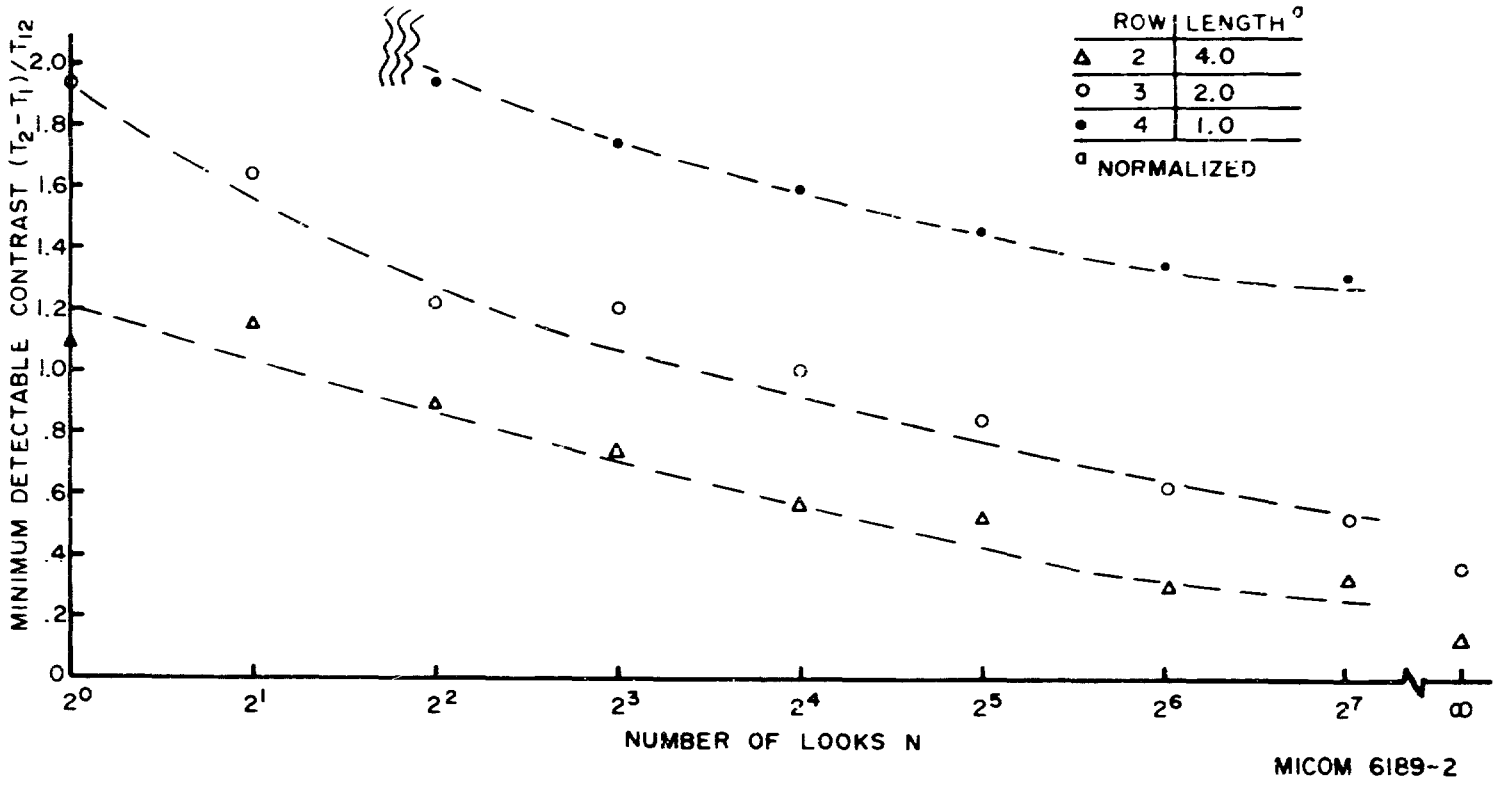

Figure 10. Object contrast required for detection of three different size test pattern discs as a function of the number of superimposed independent speckled images, N. (The speckle size is equal to the diameter of the discs in row 4.)

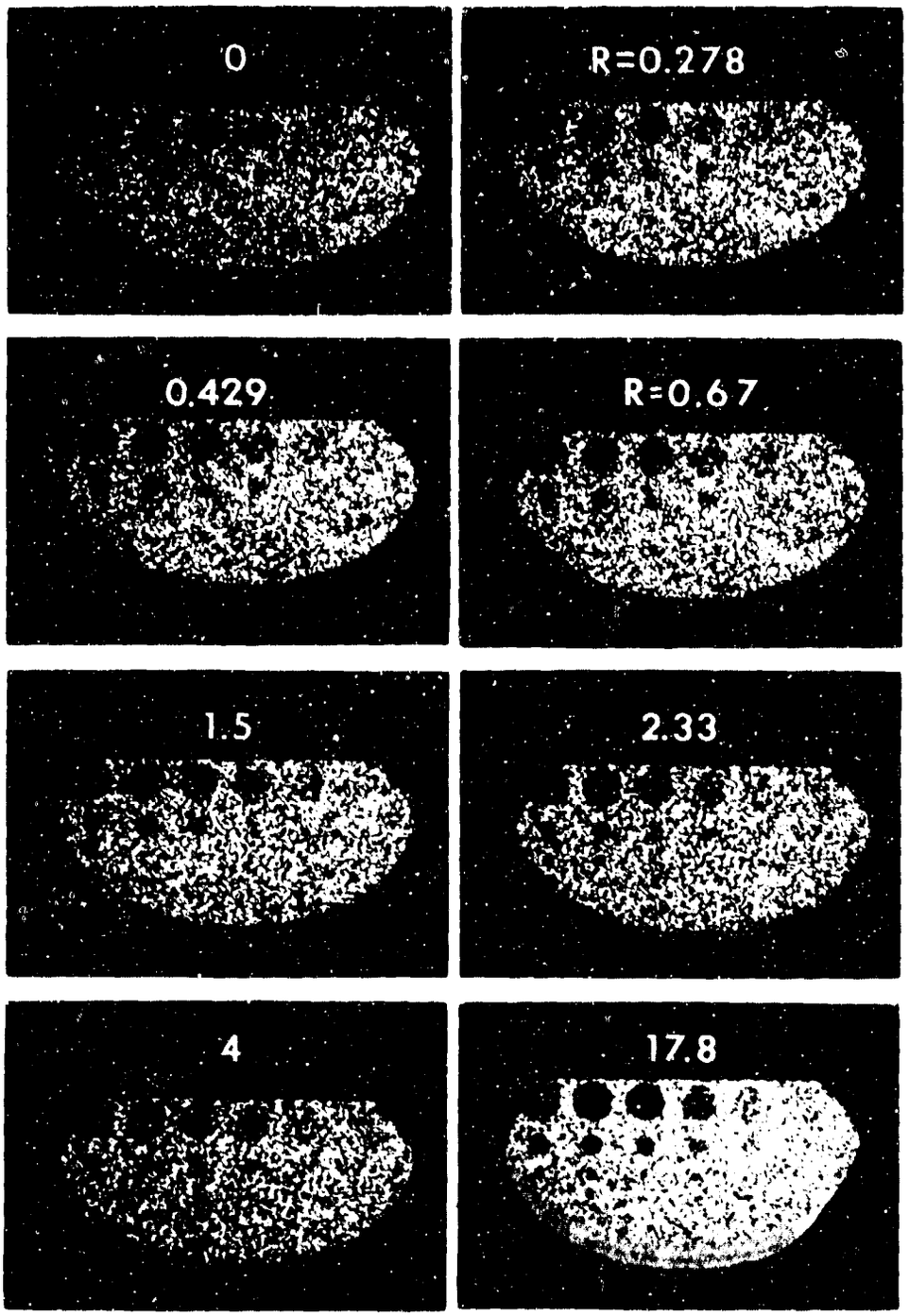

MICOM 6216-3

Figure 11. Test pattern images of columns 1-6, with plate formed by illumination with a plane wave and a diffuse beam.

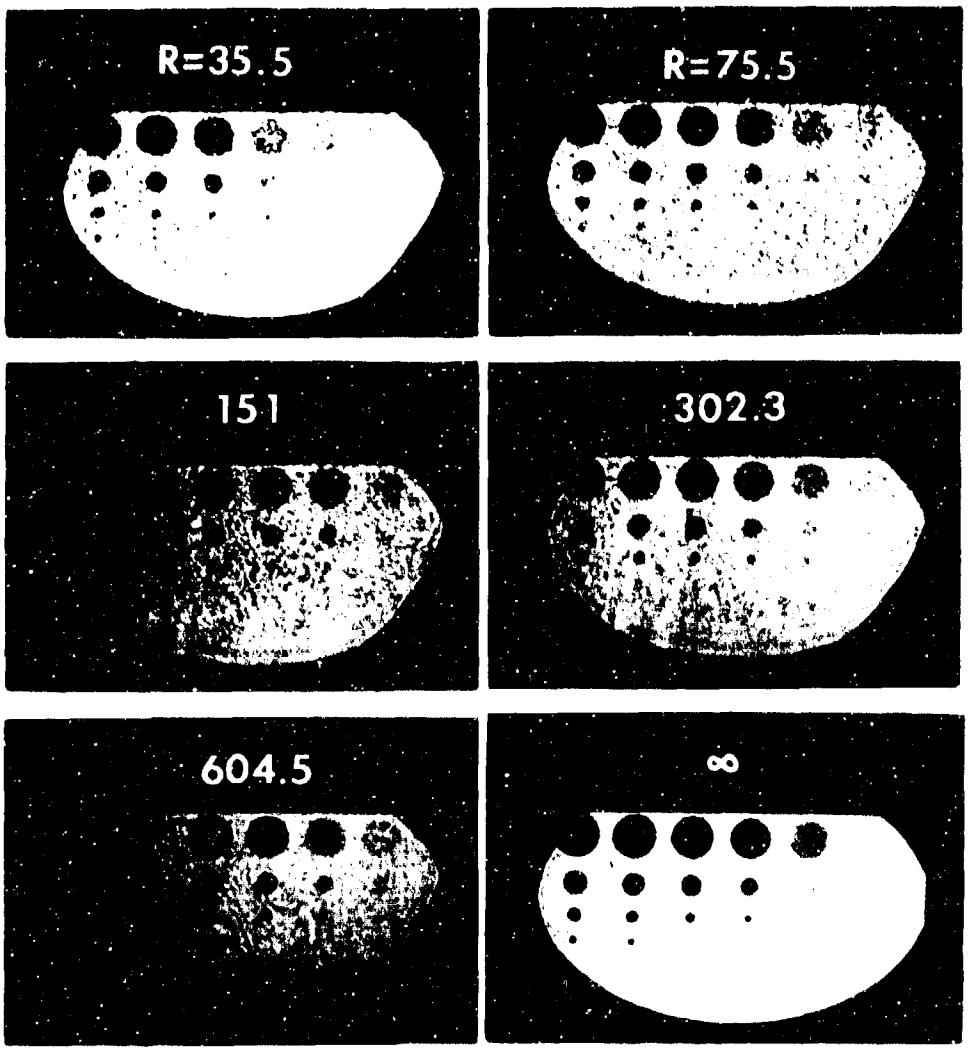

Figure 11. (Concluded.)

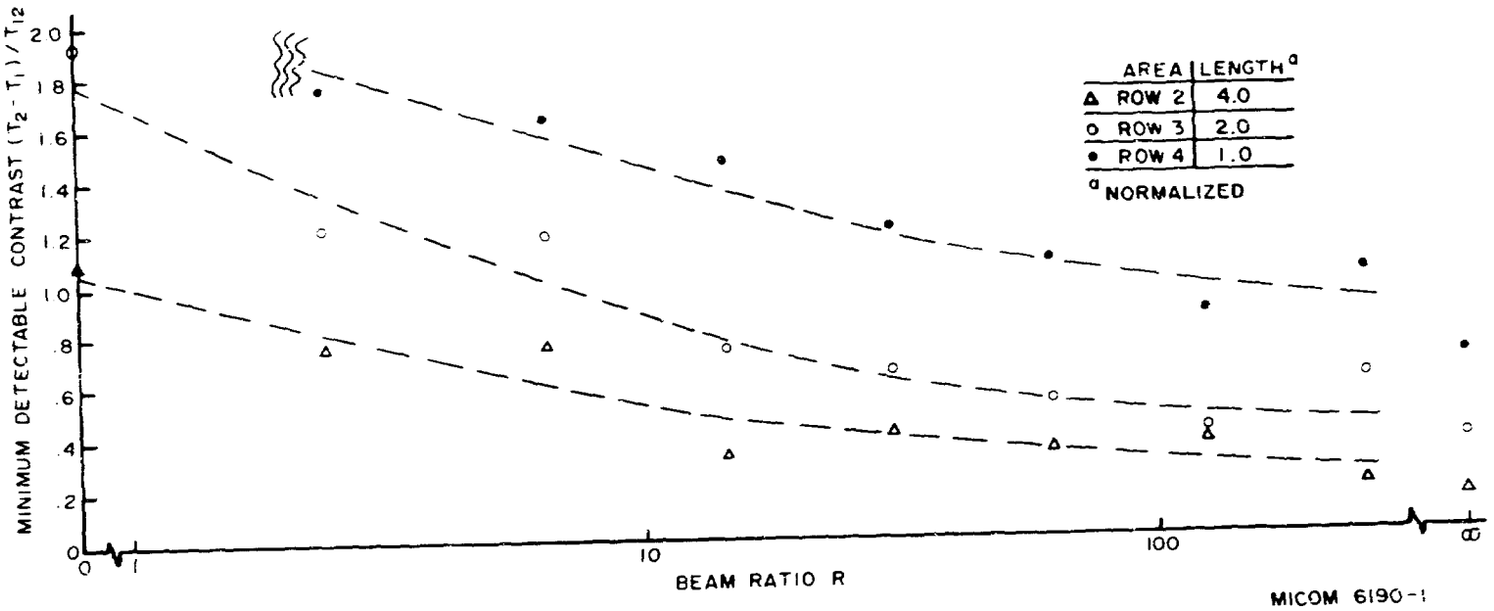

Figure 12. **Object contrast required for detection of test pattern discs of the different sizes as a function of the ratio of intensities, R, of the plane wave component to the diffuse component of the illuminating beam. (The speckle size is approximately equal to the diameter of the discs in row 4.)**

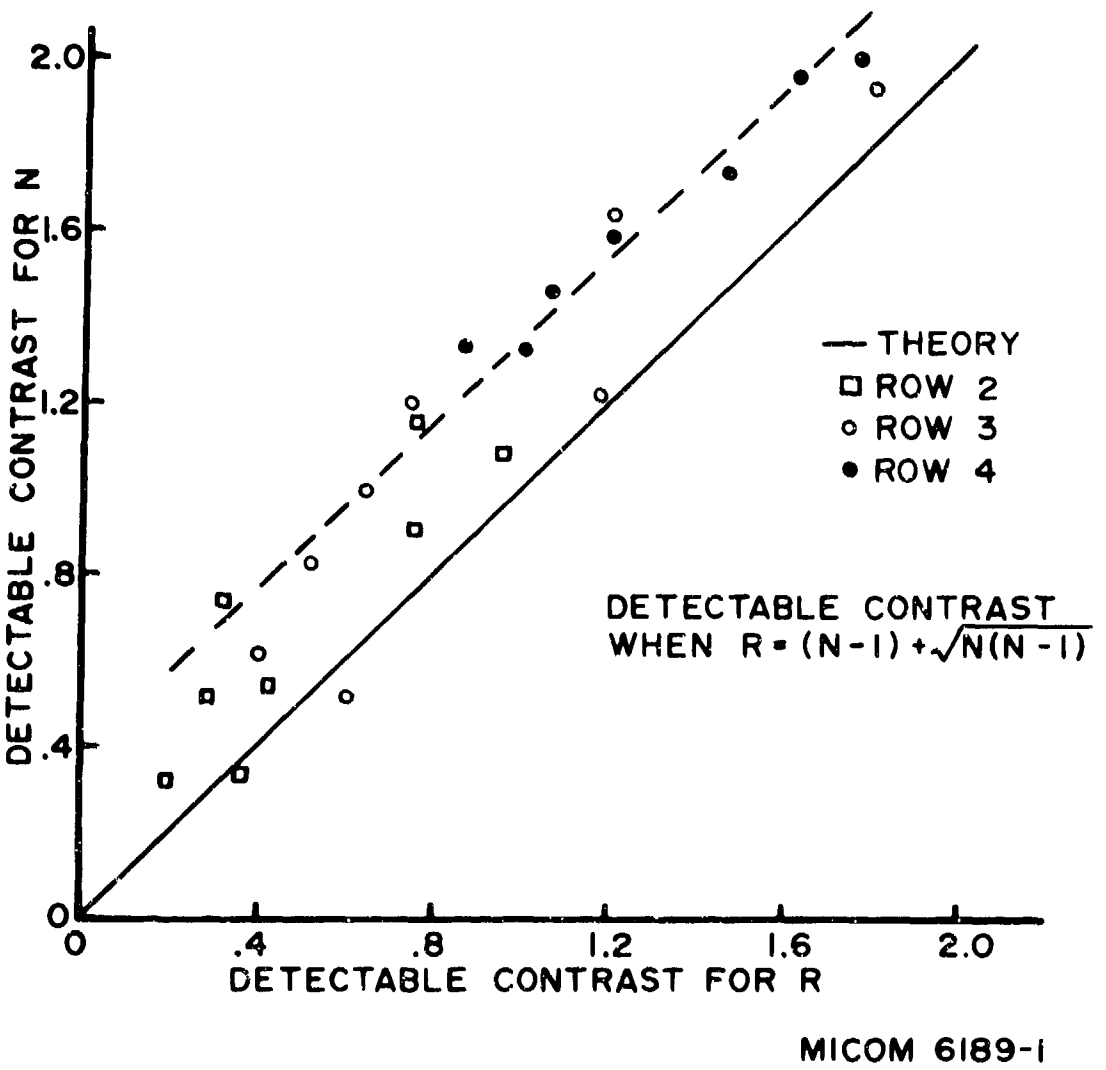

Figure 13. Comparison of minimum detectable contrast for images formed by N independent speckle field superpositions with the minimum detectable contrast for images formed by illumination with the equivalent ratio of plane wave to diffuse beam intensity given by Equation (25).

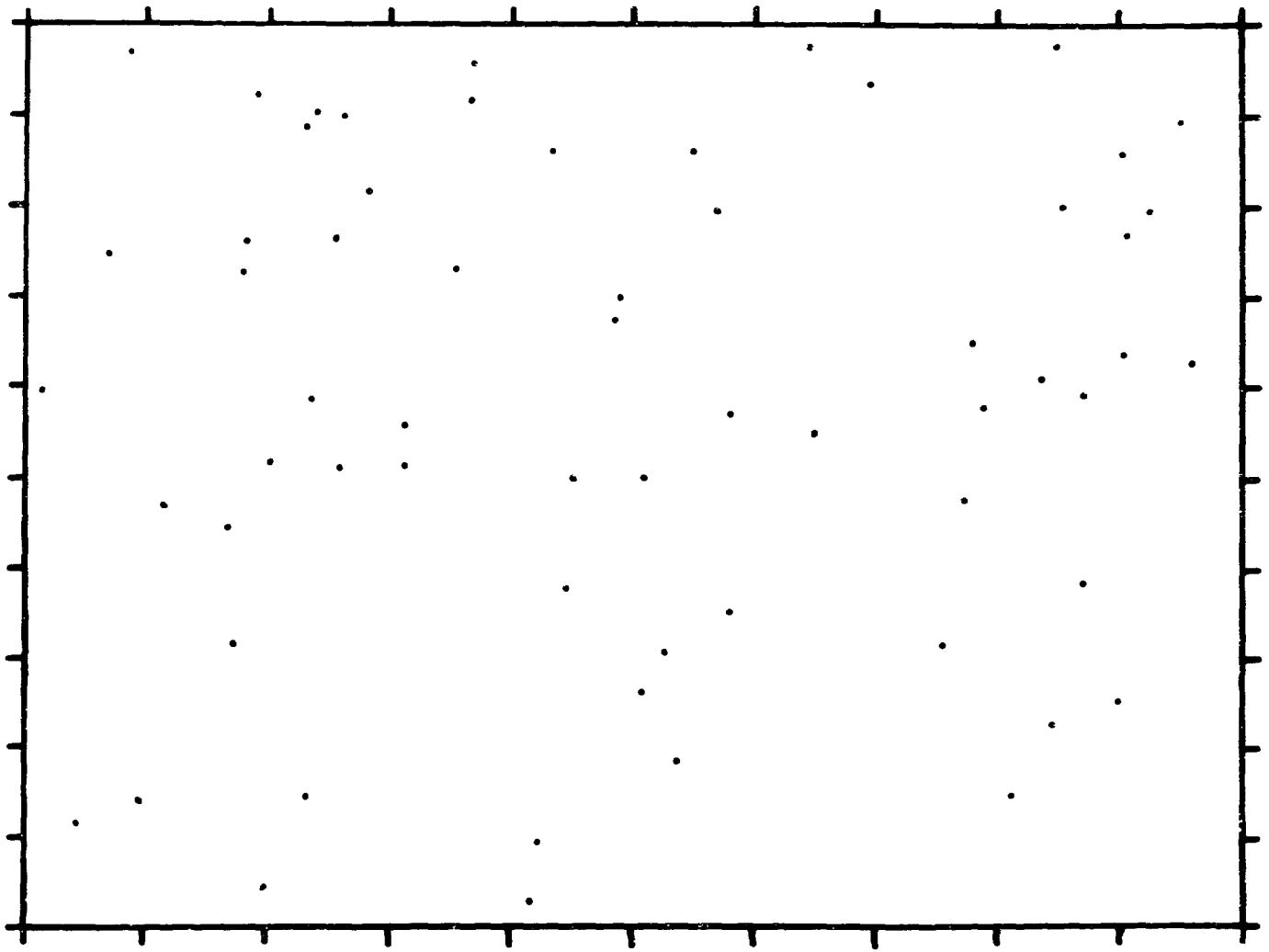

Figure 14. Random two-dimensional array. MICOM 6217-2

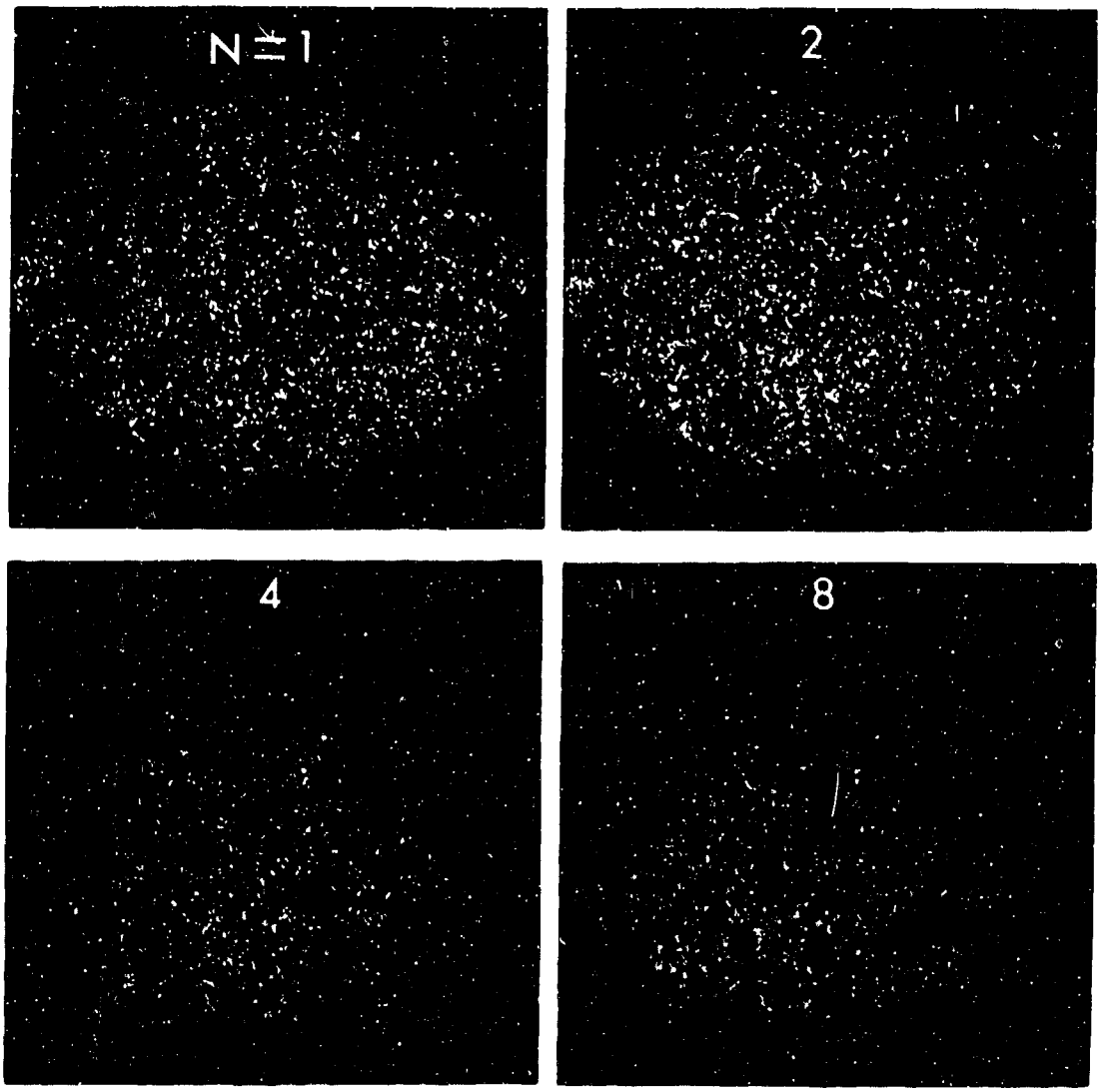

Figure 15. Images of high-contrast, 1.77-mm-diameter disc array with speckle averaged by superposition of N speckle patterns. (Contrast 1.97.)

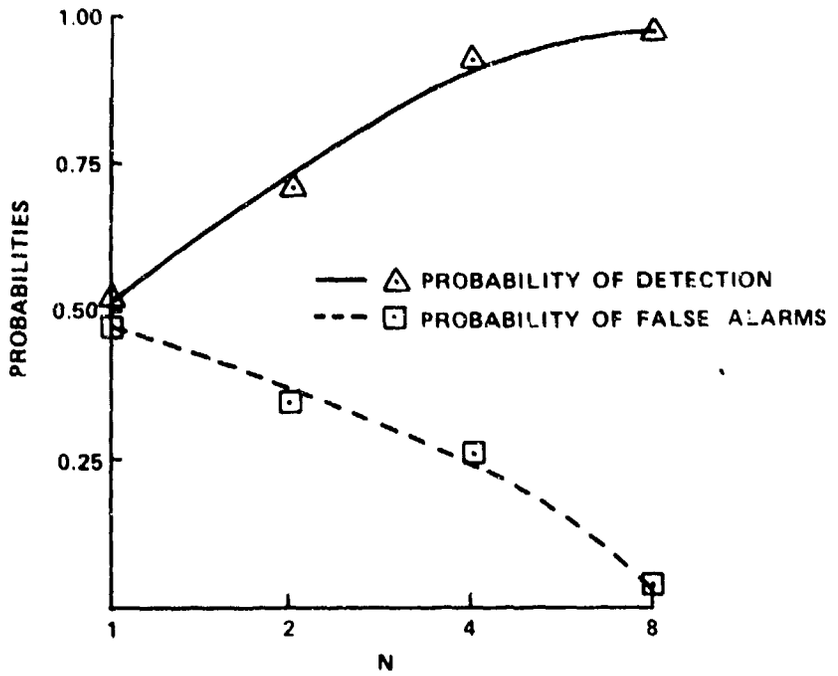

Figure 16. High-contrast disc detection in a random array. The disc diameter is approximately three times the speckle size.

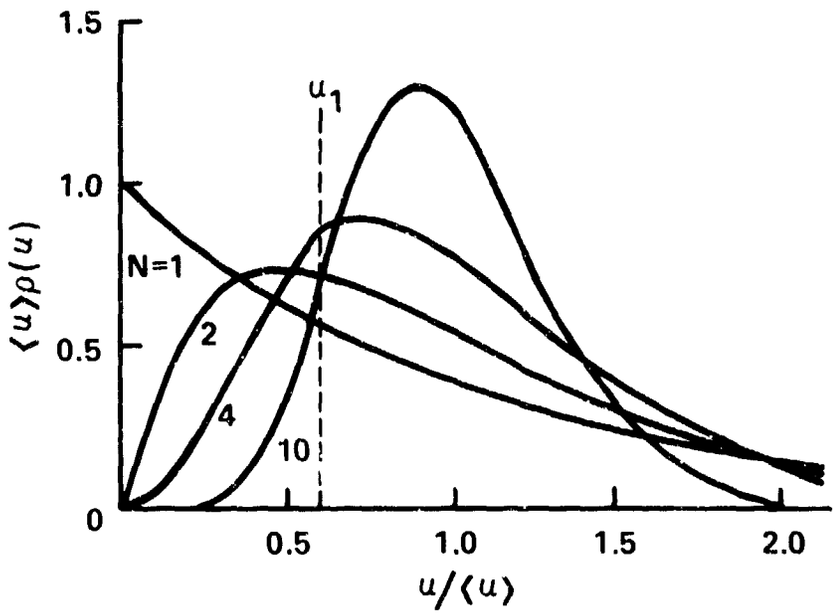

Figure 17. Probability density of speckle intensity (Reference 4, p. 54).

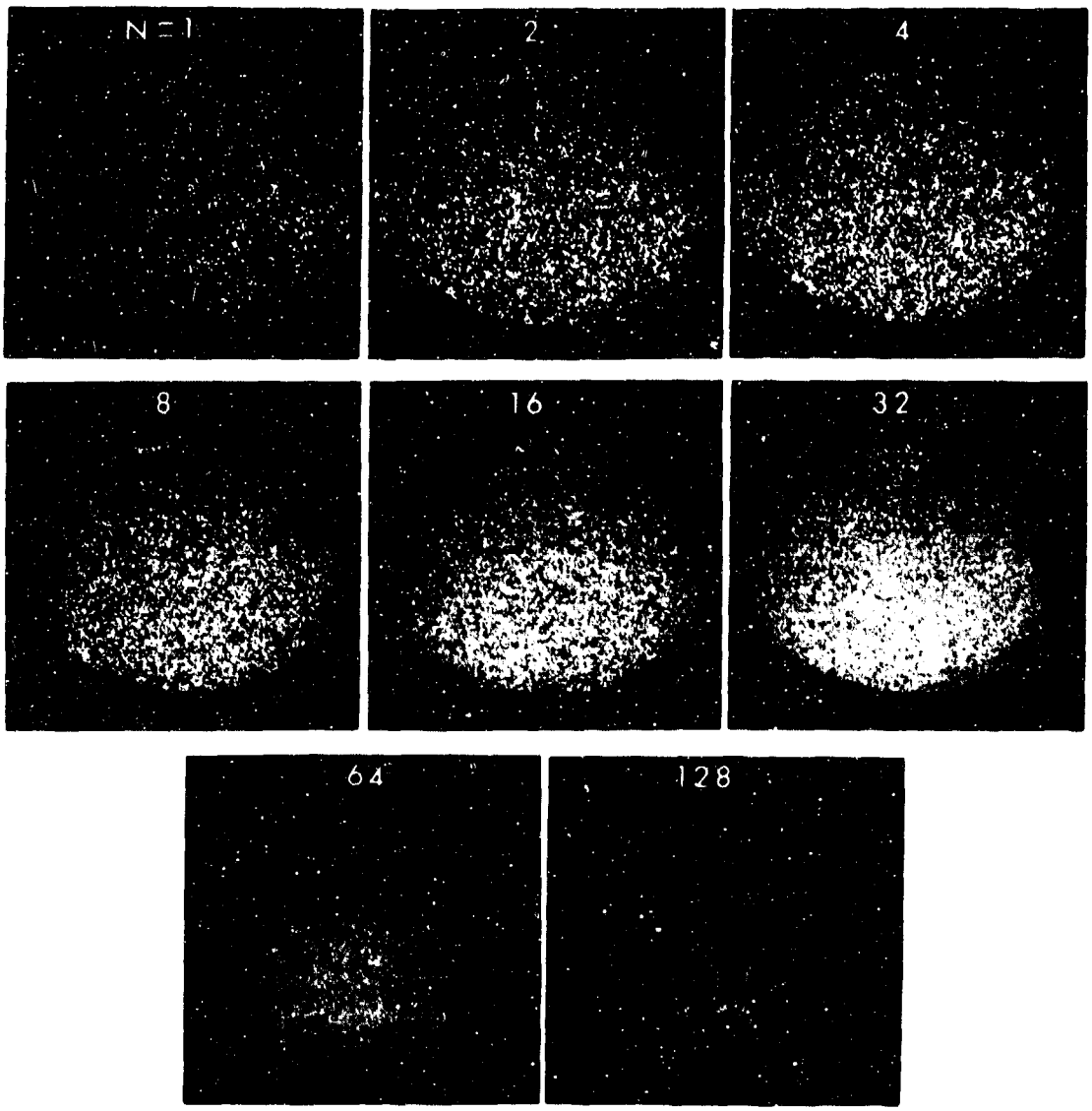

Figure 18. Images of low-contrast 1.77-mm-diameter disc array with speckle averaged by N speckle pattern superposition. (Contrast 0.23.)

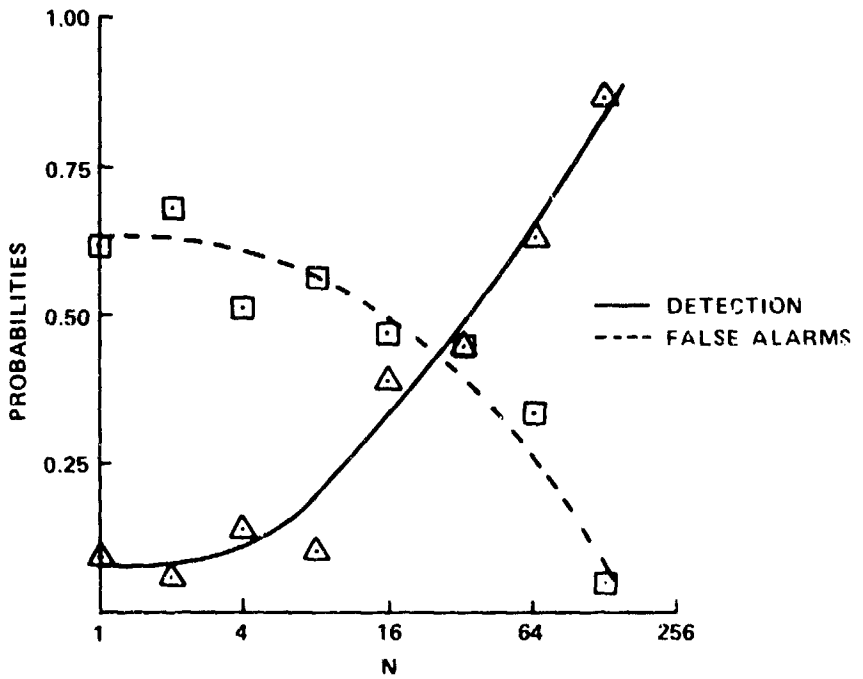

Figure 19. Low-contrast disc detection in a random array. The disc diameter is approximately three times the speckle size.

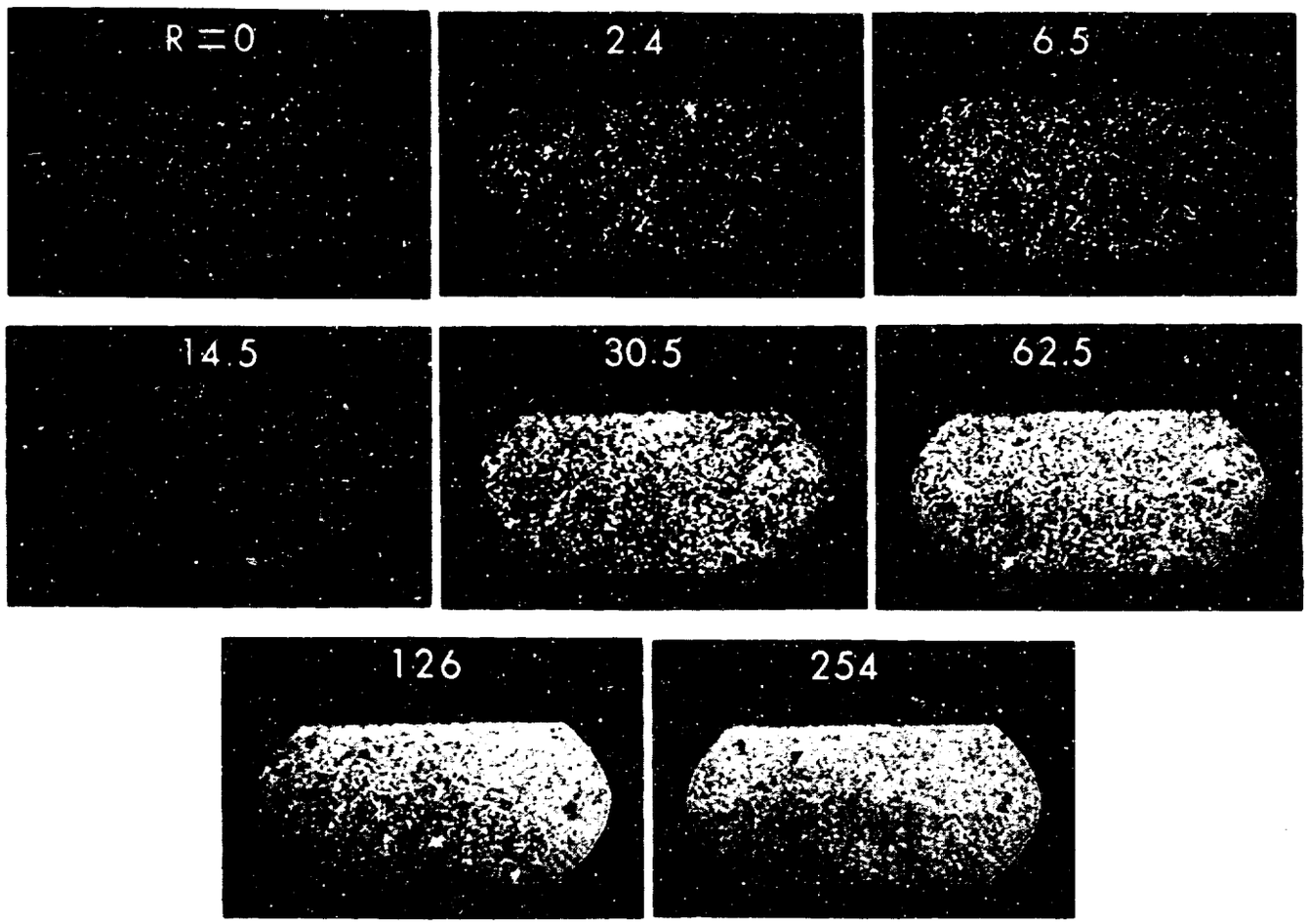

Figure 20. Images of low-contrast 1.77-mm-diameter disc arrary with plane wave and diffuse beam ratios, R, corresponding to values of N in Figure 18.

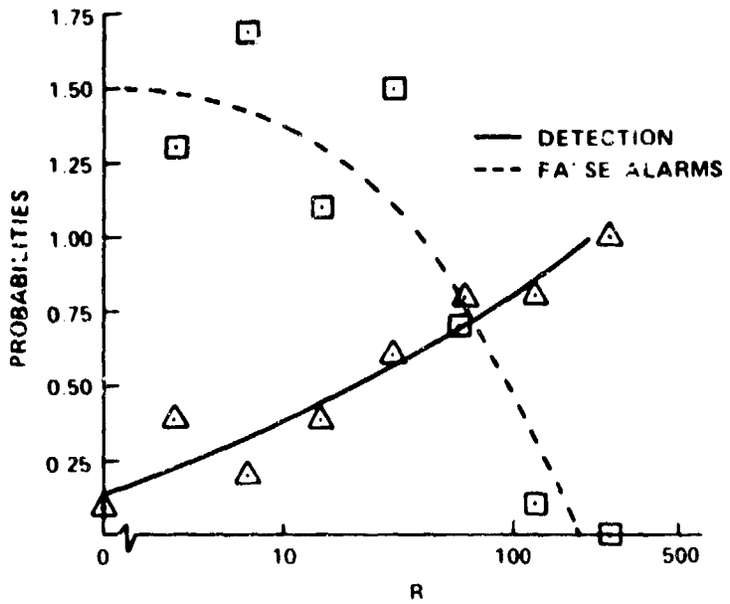

Figure 21. Low-contrast disc detection in a random array. The disc diameter is approximately three times the speckle size.

DISTRIBUTION

	No of Copies
Commander Defense Documentation Center Attn DDC-TCA Cameron Station Alexandria, VA 22314	12
Commander US Army Research Office Attn Dr R Lontz P O Box 12211 Research Triangle Park, NC 27709	2
US Army Research and Standardization Group (Europe) Attn DRXSN-E-RX, Dr Alfred K Nedoluha Box 65 FPO, New York 09510	2
US Army Material Development and Readiness Command Attn Dr Gordon Bushy Dr James Bender Dr Edward Sedlak 5001 Eisenhower Avenue Alexandria, VA 22333	1 1 1
Headquarters Hq DA (DAMA-ARZ) Washington D C 20301	2
Director of Defense Research and Engineering Engineering Technology Attn Mr L Weisberg Washington, D C 20301	2
Director Defense Advanced Research Project Agency STO Attn Commander T F Wiener D W Walsh 1400 Wilson Boulevard Arlington VA 22209	1 1
Commander US Army Aviation Systems Command 12th and Spruce Streets St Louis MO 63166	1
Director US Army Air Mobility Research and Development Laboratory Ames Research Center Moffett Field, CA 94035	1
Commander US Army Electronics Research & Development Command Attn DRSEL-TL-T, Dr Jacobs DRSEL-CT, Dr R Buser DELEW-E, Henry E Sonntag Fort Monmouth, NJ 07703	1 1 1
Director US Army Night Vision Laboratory Attn John Johnson Mr John Deline Mr Peter VanAtta Fort Belvoir, VA 22060	1 1 1
Commander US Army Picatinny Arsenal Dover, NJ 07801	1
Commander US Army Harry Diamond Laboratories 2800 Powder Mill Road Adelphi, MD 20783	1
Commander US Army Foreign Science and Technology Center Attn W S Alcott Federal Office Building 220 7th Street NE Charlottesville VA 22901	1
Commander US Army Training and Doctrine Command Fort Monroe, VA 22351	1
Director Ballistic Missile Defense Advanced Technology Center	

	No of Copies
Attn ATC-D	1
ATC-O	1
ATC-R	1
ATC-T	1
P O Box 1500 Huntsville, AL 35808	
Commander US Naval Air Systems Command Missile Guidance and Control Branch Washington, D C 20360	1
Chief of Naval Research Department of the Navy Washington, D C	1
Commander US Naval Air Development Center Warminster, PA 18974	1
Commander US Naval Ocean Systems Center Code 6003 Dr Harper Whitehouse San Diego CA 92152	1
Director Naval Research Laboratory Attn Dave Ringwolt	1
Code 5570 T Giaiborinzi	1
Washington D C 20390	
Commander Rome Air Development Center US Air Force Attn James Wasielewski IRRC Griffiss Air Force Base NY 13440	1
Commander US Air Force AFOSR NE Attn Dr J A Neff Building 410 Bolling Air Force Base Washington D C 20332	1
Commander US Air Force Avionics Laboratory Attn D Rees	1
W Schoonover	1
Dr E Champaign	1
Dr J Ryles	1
Gale Urban	1
David L Flannery	1
Wright Patterson Air Force Base OH 45433	
Commander AFATL LMT Charles Warren Eglin Air Force Base FL 32544	1

	No of Copies
Environmental Research Institute of Michigan Radar and Optics Division Attn Dr A Kozma	1
Dr C C Aleksoff	1
Juris Upatnieks	1
P O Box 618 Ann Arbor MI 41807	
IIT Research Institute Attn GACIAC 10 West 35th Street Chicago IL 60616	1
Dr J G Castle Physics Department University of Alabama 4701 University Drive N W Huntsville AL 35807	1
Science and Technology Division Institute of Defense Analysis Attn Dr Vincent J Corcoran 400 Army-Navy Drive Arlington VA 22202	1
Optical Science Consultants Attn Dr D L Fried P O Box 388 Yorba Linda, CA 92686	1
Commander Center for Naval Analyses Attn Document Control 1401 Wilson Boulevard Arlington, VA 22209	1
Raytheon Company Attn A V Jelalian 528 Boston Post Road, Sudbury, MA 01776	1
Dr J W Goodman Information Systems Laboratory Department of Electrical Engineering Stanford University Stanford CA 94305	1
Eric G Johnson Jr National Bureau of Standards 325 S Broadway Boulder CO 80302	1
M Vanderlind Battelle Columbus Labs 505 King Ave Columbus OH 43201	1

	No of Copies
Dr Nicholas George The Institute of Optics University of Rochester Rochester, NY 14627	1
DRDMI-T, Dr Kobler	1
James Fagan	1
DRDMI-H, Dr J P Hallowes, Jr	1
DRCPM-PE	1
DRDMI-NS, Jerry Hagood	1
DRDMI-TE, W Pittman	1
Lewis G Minor	1
DRDMI-TG	1
TG, James A McLean	1
TD	3
TB	1
DRDMI-C	1
DRDMI-Y	1
DRDMI-TR, Dr R L Hartman	1
Dr J S Bennett	1
Dr C R Christensen	1
Dr B D Guenther	1
Dr J L Smith	1
Dr J D Stettler	1
DRDMI-TI (Reference Copy)	1
-TI (Record Set)	1
DRDMI-TRO	60
DRDMI-TBD	3
DRCPM-PE-E, John Pettitt	1
DRSMI-LP, Mr Voigt	1
Naval Avionics Facility Indianapolis, IN 46218	1
F B Rotz Harris Corp P O Box 37 Melbourne, FL 32901	1
Robert L Kurtz TAI Corp 8302 Whitesburg Dr, S E Huntsville, AL 35802	1
J R Vyce Itek Corp 10 Maguire Road Lexington, MA 02173	1
Dr David Casasent Carnegie Mellon University Hamerschage Hall Rm 106 Pittsburgh, PA 15213	1
David M Karnes McDonnell Douglas Astronautics 5301 Bolsa Ave Huntington Beach, CA 92647	1
Prof Anil K Jain Dept of Elec Engr University of California, Davis Davis, CA 95616	1
Gerald B Brandt Westinghouse Electric Corp Research and Development Center Pittsburgh, PA 15235	1
K G Leib Research Department Grumman Aerospace Corp Bethpage, NY 11714	1
Terry Turpin Dept of Defense 9800 Savage Road Ft George G Meade, MD 20755	1
Dr Stuart A Collins Electrical Engineering Dept Ohio State University 1320 Kennear Rd Columbus, OH 43212	1
Mike Scarborough, MS-19 Teledyne Brown Engineering Cummings Research Park Huntsville, AL 35807	1
Commander AFEL Hanscom Air Force Base, MD 01731	1
Dr Arthur N Chester	1
Dr Donald H Closs	1
Thomas R O'Meara	1
Dr Wilfried O Eckhardt Hughes Research Laboratories 3011 Malibu Canyon Road Malibu, CA 90265	1
H J Caulfield Aerodyne Research, Inc Bedford Research Park Crosby Drive Bedford, MA 01730	1
TRW Defense & Space Systems Group One Space Park Attn Dr Peter O Clark Redondo Beach, CA 90278	1

☆U.S. GOVERNMENT PRINTING OFFICE 1979—640-122/607 REGION NO.4